

CZECH TECHNICAL UNIVERSITY IN PRAGUE

Faculty of Electrical Engineering

Department of Telecommunication

**Coexistence of optical systems on
a physical layer**

May 2018

Bc. Jan Brychta

Supervisor: Ing. Michal Lucki, Ph.D.

Declaration

I hereby declare that I wrote the master's thesis by myself under the careful supervision of my thesis supervisor and I have used only the literature mentioned in the reference list. I also declare that I agree with lending or publishing my work with the consent of the department.

Date: 11.05.2018

.....

Signature

Prohlášení

Prohlašuji, že jsem zadanou diplomovou práci zpracoval sám s přispěním vedoucího práce a používal jsem pouze literaturu v práci uvedenou. Dále prohlašuji, že nemám námitek proti půjčování nebo zveřejňování mé diplomové práce nebo její části se souhlasem katedry.

Datum: 11.05.2018

.....

Podpis



ZADÁNÍ DIPLOMOVÉ PRÁCE

I. OSOBNÍ A STUDIJNÍ ÚDAJE

Příjmení: **Brychta** Jméno: **Jan** Osobní číslo: **411199**
Fakulta/ústav: **Fakulta elektrotechnická**
Zadávací katedra/ústav: **Katedra elektromagnetického pole**
Studijní program: **Elektronika a komunikace**
Studijní obor: **Radiová a optická technika**

II. ÚDAJE K DIPLOMOVÉ PRÁCI

Název diplomové práce:

Koexistence více optických systémů na fyzické vrstvě

Název diplomové práce anglicky:

Coexistence of More Optical Systems at the Physical Layer

Pokyny pro vypracování:

Cílem práce je studium možností současného provozování více optických systémů na společné fyzické vrstvě za různých podmínek zatížení sítě. Důležitým cílem je porovnání integrace systémů o různých rychlostech, různé kanálové roztači nebo používajících odlišné modulační technologie (CWDM, DWDM, PON, AON a další). Simulace provádějte v prostředí Optisim a s ohledem na doporučení ITU-T v této oblasti. Finálním výsledkem jsou modely koexistence různých přenosových systémů a prostředků a teoretické úvahy o tom, které systémy a za jakých podmínek lze pomyslně slučovat a u kterých systémů či variant nasazení se tento postup nedoporučuje.

Seznam doporučené literatury:

- [1] ITU-T G-series Supplement 39: Transmission systems and media, digital systems and networks. ITU, 2012.
- [2] Chandrasekhar, S., Liu, X., Fauconnier, T., Charlet, G., Bigo, S.: Impact of Channel Plan and Dispersion Map on Hybrid DWDM Transmission of 42.7-Gb/s DQPSK and 10.7-Gb/s OOK on 50-GHz Grid. IEEE Photonics Technology Letters. IEEE, 2007.
- [3] Udalcovs, A., Monti, P., Bobrovs, V., Schatz, R., Wosinska, L., Ivanovs, G.: Spectral and energy efficiency considerations in mixed-line rate WDM networks with quality guarantee. 2013 15th International Conference on Transparent Optical Networks (ICTON). IEEE, 2013.

Jméno a pracoviště vedoucí(ho) diplomové práce:

Ing. Michal Lucký, Ph.D., katedra telekomunikační techniky FEL

Jméno a pracoviště druhé(ho) vedoucí(ho) nebo konzultanta(ky) diplomové práce:

Datum zadání diplomové práce: **18.01.2018**

Termín odevzdání diplomové práce: _____

Platnost zadání diplomové práce: **30.09.2019**

Ing. Michal Lucký, Ph.D.
podpis vedoucí(ho) práce

podpis vedoucí(ho) ústavu/katedry

prof. Ing. Pavel Řířka, CSc.
podpis děkana(ky)

III. PŘEVZETÍ ZADÁNÍ

Diplomant bere na vědomí, že je povinen vypracovat diplomovou práci samostatně, bez cizí pomoci, s výjimkou poskytnutých konzultací. Seznam použité literatury, jiných pramenů a jmen konzultantů je třeba uvést v diplomové práci.

17.5.2018

Datum převzetí zadání

Podpis studenta

Summary

The purpose of the thesis is to analyze the possibilities of optical systems coexistence on a shared physical layer. The interactions between optical systems utilising various modulation formats are investigated and conclusions about optical system design and transition to higher bitrate are made. Those conclusions are supported by the simulation results made with the help of the OptSim simulation software.

Keywords:

DWDM, Hybrid systems, Coexistence, Modulation formats, Optical fiber communication

Anotace

Cílem této práce je prozkoumat možnosti koexistence optických přenosových systémů na jedné fyzické vrstvě. Je zkoumána interakce mezi optickými systémy využívajícími různé modulační formáty a jsou vyvozeny závěry ohledně návrhu optických systémů a přechodu na vyšší rychlosti, které se opírají o výsledky simulací prováděných za pomoci programu OptSim.

Klíčová slova:

DWDM, Hybridní systémy, Koexistence, Modulační formáty, Optické vláknové sítě
OptSim

Acknowledgement

I would like to express my gratitude to my supervisor Ing. Michal Lucki, Ph.D. for his guidance, valuable advice and his patience. I would also like to thank my family and my friends for their continuous support throughout my studies.

Table of Contents

1 INTRODUCTION.....	11
1.1 PROBLEM STATEMENT.....	11
1.2 THESIS STRUCTURE.....	12
2 STATE OF THE ART.....	13
2.1 WAVELENGTH DIVISION MULTIPLEXING.....	13
2.1.1 CWDM.....	13
2.1.2 DWDM.....	14
2.2 SIGNAL REGENERATION.....	14
2.2.1 Dispersion compensation.....	14
2.2.2 EDFA.....	15
2.3 NON-LINEAR EFFECTS.....	16
2.4 CHANNEL COEXISTENCE.....	17
3 METHODS.....	18
3.1 TIME DOMAIN SPLIT-STEP.....	18
3.2 BER.....	18
3.3 Q-FACTOR.....	20
3.4 MODULATIONS.....	22
3.4.1 NRZ-OOK.....	22
3.4.2 DPSK.....	23
3.4.3 DQPSK.....	24
3.5 SIMULATION LAYOUTS.....	25
4 RESULTS.....	29
4.1 CHANNEL PROPERTIES.....	29
4.1.1 Attenuation.....	29
4.1.2 Dispersion.....	30
4.2 ADDING NEW CHANNELS TO AN EXISTING SYSTEM.....	32
4.2.1 System with mixed channel groups.....	32
4.2.2 Interference caused by DPSK modulation.....	37
4.2.3 Interference caused by DQPSK modulation.....	38
4.2.4 System with separated channel groups.....	40
4.2.5 Transitioning to a new system.....	43
5 CONCLUSION.....	46
BIBLIOGRAPHY.....	49

List of Figures

Fig. 2.1: WDM network architecture.....	13
Fig. 2.2: FWM induced distortions in WDM systems: a) equal channel spacing, b) unequal channel spacing [25].....	16
Fig. 3.1: BER estimate range (95% confidence interval) for BER=10 ⁻⁹ [52].....	19
Fig. 3.2: Determining the Q-factor.....	20
Fig. 3.3: Q-factor estimate range (95% confidence interval) for Q=15.56 dB, corresponding to BER=10 ⁻⁹ [52].....	21
Fig. 3.4: a) OOK modulation constellation diagram, b) NRZ-OOK eye diagram.....	22
Fig. 3.5: NRZ-OOK transmitter implementation.....	22
Fig. 3.6: DPSK modulation constellation diagram, b) DPSK eye diagram.....	23
Fig. 3.7: DPSK transmitter implementation.....	23
Fig. 3.8: a) (D)QPSK modulation constellation diagram, b) Instantaneous phase deviation of a DQPSK signal.....	24
Fig. 3.9: DQPSK transmitter implementation.....	24
Fig. 3.10: Optical network layout with repeated signal regeneration.....	25
Fig. 3.11: a) Dispersion, b) power of a signal propagating through the network.....	26
Fig. 3.12: DWDM transmitter array – DQPSK modulation.....	26
Fig. 3.13: Repeated segment with dispersion compensation and EDFA.....	27
Fig. 3.14: DWDM receiver array – DQPSK modulation.....	27
Fig. 3.15: Example of a used simulation layout – coexistence of an OOK and a DQPSK DWDM system.	28
Fig. 4.1: Impact of distance between EDFA segments on a) BER, b) Q-factor.....	29
Fig. 4.2: Optical power a) transmitted, b) at 10 km, c) at 50 km.....	30
Fig. 4.3: Dispersion compensation: a) none, b) partial, c) full compensation.....	31
Fig. 4.4: Interleaved DWDM channels.....	32
Fig. 4.5: Frequency spectrum of interleaved DWDM system.....	33
Fig. 4.6: The effects of adjacent channel interference.....	34
Fig. 4.7: Adjacent channel interference impact on a) 40 Gbps channel, b) 60 Gbps..	35
Fig. 4.8: Adjacent channel interference for 10 DWDM channels.....	35
Fig. 4.9: Differences in the effect of interference based on channel spacing.....	36
Fig. 4.10: Interference caused by DPSK channels.....	37
Fig. 4.11: BER of 10 Gbps OOK channels affected by DQPSK channel crosstalk....	38
Fig. 4.12: BER of 20 and 40 Gbps OOK channels affected by DQPSK channel crosstalk.....	39
Fig. 4.13: Separated channel groups.....	40
Fig. 4.14: Finding the optimal frequency spacing.....	41
Fig. 4.15: Channel crosstalk at three different channel spacings.....	40
Fig. 4.16: The relationship between frequency spacing and bit error rate.....	42
Fig. 4.17: OOK channel affected by various sources of interference.....	43
Fig. 4.18: Added channels affected by the old OOK system.....	44

List of Abbreviations and Symbols

APSK	Amplitude and Phase-Shift Keying
BER	Bit Error Rate
CD	Chromatic Dispersion
CFBG	Chirped Fiber Bragg Grating
CWDM	Coarse Wavelength Division Multiplex
DCF	Dispersion Compensating Fiber
DCM	Dispersion Compensating Module
DPSK	Differential Phase-Shift Keying
DQPSK	Differential Quadrature Phase-Shift Keying
DWDM	Dense Wavelength Division Multiplex
EDFA	Erbium-Doped Fiber Amplifier
FFT	Fast Fourier Transform
FWM	Four-Wave Mixing
MOF	Micro-Structured Optical Fiber
NRZ	Non-Return-to-Zero
OOK	On-Off-Keying
OSNR	Optical Signal-to-Noise Ratio
QoS	Quality of Service
SBS	Stimulated Brillouin Scattering
SMF	Single-Mode Fiber
SPM	Self-Phase Modulation
SRS	Stimulated Raman Scattering
SSFM	Split-Step Fourier Method
TDSS	Time-Domain Split-Step
WDM	Wavelength Division Multiplexing
XPM	Cross-Phase Modulation

1 Introduction

With increasing popularity of cloud-based services such as Netflix, Amazon Prime and Spotify and the associated growth of bandwidth demands, it becomes a challenge for network operators to upgrade the network while keeping important resources like cost and energy consumption to minimum values. Since replacing the entire network infrastructure isn't economically feasible, gradual transition to a new system as traffic grows is the logical solution [1].

This can be done by either adding new optical channels to the existing system or replacing existing channels with higher bitrate channels. In practical applications, the replacement of channels is done in several steps in order to prevent a temporary loss of service or keep it to minimum [2]. First, the new channel group is added to the system, with its total bitrate at least equal to the old system. After that, the added channels transmission quality is analyzed and the channels are set up for transmission. Finally, the service is switched from the old channels onto the new ones. After the new system is in place, the old channels can be either kept for extra bandwidth or discarded without any significant loss of service. The gradual transition also ensures that if any problems with the new channels occur, the network operator can rollback to the still present old system.

1.1 Problem statement

This thesis explores the coexistence of optical systems on a physical layer during the transitional period when multiple channels with different bitrates and modulation formats interact with each other, shows the problems that may arise from cross-channel interaction and proposes possible solutions. Most WDM systems utilise 10 Gbps channels with amplitude modulation. The NRZ-OOK modulation does not perform well at bitrates higher than 40 Gbps, therefore other modulation formats have to be utilised. Transition to higher bitrates or more advanced modulations requires taking into account the changes in transmission quality resulting from non-linear effects as well as more strict dispersion requirements. The transmission properties of a channel affected by WDM crosstalk are very different from those of a solitary channel and they largely depend not only on the channel itself, but also on the neighboring channel properties. The cross-channel interference caused by the neighboring channels plays a major role in determining the transmission quality, especially if the channels

in question are using phase modulation format. The impact of using different modulations on transmission quality when adding new channels into the system is presented in the thesis, as well as the effects of dispersion, attenuation and the frequency of signal regeneration or the channel spacing.

1.2 Thesis structure

The second chapter presents the state of the art, gives the theoretical background and general overview on the components and techniques used. The third chapter presents the methods used in making the thesis. The time-domain split-step method used for simulating the channel behaviour is explained, the channel parameters which were used for determining the transmission quality are introduced as well as the modulation formats and their implementation in the OptSim simulation software. Finally, the simulation layouts are shown and explained. The fourth chapter contains all the performed simulations and their results, first part of the chapter deals with the general channel properties and the second part focuses on cross-channel interaction in regards to the channel bitrates, modulations used as well as channel spacing. The final chapter discusses the results shown in the previous chapter and their implications, the methodology behind the implementation of new channels is proposed and the possible problems that may occur are mentioned. The final chapter concludes with thoughts on the possible limitations of the project and potential further areas of study.

2 State of the Art

2.1 Wavelength Division Multiplexing

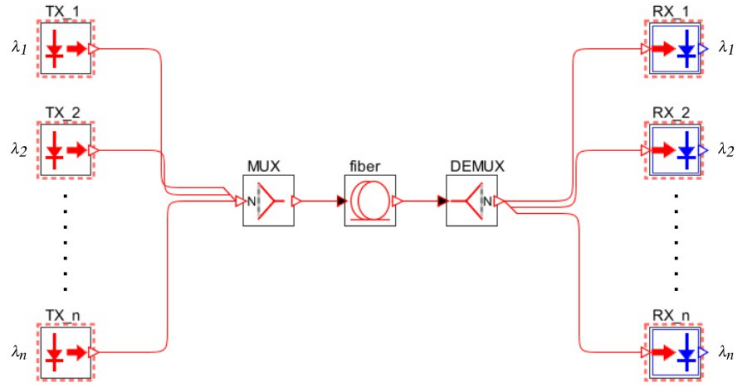


Fig. 2.1: WDM network architecture.

Wavelength Division Multiplexing (WDM) is employed in order to increase the system capacity. Each channel operates on a different wavelength, allowing multiple channels to coexist on a physical layer [3][4]. The basic topology of a WDM network is shown in Figure 2.1. The optical network consists of multiple transceivers (TX_1 to TX_n), each operating on a different frequency. The signals are multiplexed and propagate through a shared optical fiber. After demultiplexing, each signal is detected by its respective receiver (RX_1 to RX_n). The total system bitrate is calculated as:

$$B_T = B_1 + B_2 + \dots + B_N \quad (1)$$

where B_T is the total bitrate and B_i is the bitrate of the i^{th} channel [5].

2.1.1 CWDM

Coarse Wavelength Division Multiplexing (CWDM) is characterised by wider channel spacing than Dense WDM described in the chapter below. CWDM systems are often utilised in cost-efficient applications thanks to its wavelength selection tolerances and wide passband filters [6]. 18 CWDM channels are defined by ITU-T, ranging from 1270 to 1610 nm with channel spacing of 20 nm.

2.1.2 DWDM

Dense Wavelength Division Multiplexing (DWDM) benefits from narrower channel spacing than CWDM. The channel spacings as defined in [7] are 12.5 GHz, 25 GHz, 50 GHz and 100 GHz. The nominal channel frequencies are defined as

$$f_n = 193.1 + n\Delta_f \quad (2)$$

where n is a positive or negative integer including 0 and Δ_f is the channel spacing. The differences between CWDM and DWDM systems are highlighted in [8] and the spectral efficiency of a DWDM system is thoroughly elaborated upon in [9].

2.2 Signal regeneration

2.2.1 Dispersion compensation

Chromatic dispersion (CD), analyzed in [10], is the prevalent dispersion element in single-mode fibers. Since commercial SMFs tend to have positive dispersion of around 17 ps/nm/km at 1.55 μm [11][12], dispersion compensation elements are necessary when designing a long-distance optical network, especially at higher bitrates due to low dispersion tolerance.

One method of chromatic dispersion compensation is the usage of dispersion compensating fibers (DCF). In order to regenerate the pulse shape, DCF are designed with very high negative dispersion values. micro-structured optical fiber (MOF) designs proposed in [13] offer dispersion values of up to -3290 ps/n/km at 1.55 μm . In my case, running simulations using DCF for dispersion compensation is a difficult task, because such fibers are not present in the OptSim simulation environment by default and implementing them is complicated, since many research papers do not present all fiber parameters required for proper implementation.

Another approach to dispersion compensation is using Chirped Fiber Bragg Grating (CFBG) as proposed in [14]. In [15] the superior CD compensating properties of FBG to DCF are discussed. Both methods reduce the CD to acceptable values, but DCF suffers from inserted attenuation of up to 10 dB, as opposed to CFBG added attenuation of less than 3 dB. CFBG is less susceptible to non-linear effects as well.

The dispersion slope of the dispersion compensating module (DCM) has to match the dispersion slope of the SMF used for transmission. CFBG dispersion compensation optimised for DWDM systems slope-matched with G.652 fiber is presented in [16], FBGs with long period gratings suitable for broadband (13.8 nm) systems are

discussed in [17]. The optical network utilising CFBG CD compensation is tested in [18], the optimal placement of the DCM is also explored. The CFBG is fabricated to compensate the overall dispersion of -1638 ps/nm, pre-compensation is reported to yield slightly better results than post-compensation, with inline compensation suffering from the worst bit error rate.

2.2.2 EDFA

Since transmitted optical power lowers while propagating through an optical fiber, Erbium-doped fiber amplifiers (EDFA) play a crucial role in optical signal regeneration over long distances. Signals amplified by a single or multiple EDFAs suffer from decreased OSNR caused by the amplifiers' added noise, studies show that the noise figure ranges from around 4 dB [19][20] to roughly 5 dB [21][22] in practical applications. Since my simulations will mainly consider channels at wavelength ranging from around 1540 nm to 1560 nm, both amplifier gain and noise figure can be approximated as flat values, according to [21]. The relationship between EDFA noise figure and other parameters, such as input power, is elaborated upon in [23] with noise measuring methods described in [19]. The noise and gain of optical amplifiers, however, cannot be seen as static values. The addition or the drop of channels can affect the EDFA gain, which can be detrimental to WDM network flexibility. This topic, along with countermeasures against the gain instability, is covered in [24]. This effect of EDFA gain fluctuation would be very hard to replicate in the simulation environment. Since it mostly concerns dynamic optical networks, I decided to use a fixed-gain amplifier in my simulations. When designing an optical network with multiple optical amplifiers, it is important to choose the optimal distance between each signal regeneration segment, since short regeneration intervals theoretically ensure better transmission quality, but each EDFA introduces noise into the channel. Since the inserted noise from multiple EDFAs may result in lowered transmission quality. This topic will be further explored in chapter 4.1.1.

2.3 Non-linear effects

The cross-channel interference in fiber optics is mainly caused by non-linear effects, which can be split into two types: Inflexible Stimulated Scattering, further split into Stimulated Raman Scattering (SRS) and Stimulated Brillouin Scattering (SBS), and Kerr effect. Kerr effects, the main sources of non-linear interference in WDM systems, comprise of Self-Phase Modulation (SPM), causing the frequency chirp of the transmitted signal, Cross-Phase Modulation (XPM), responsible for timing and amplitude jitter of the neighboring channels, and Four-Wave Mixing (FWM).

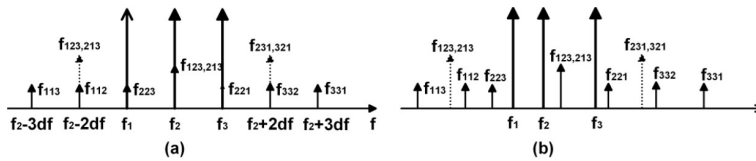


Fig. 2.2: FWM induced distortions in WDM systems: a) equal channel spacing, b) unequal channel spacing [25].

FWM is a process in which three different frequencies generate new spectral components through interaction [26]. The products are created at:

$$f_{ijk} = f_i + f_j - f_k \quad (3)$$

where f_i, f_j, f_k are the existing frequencies and f_{ijk} is the new spectral component. The creation of the new spectral components is graphically represented in Figure 2.2. In a transmission system with equal channel spacing, new spectral components overlap with the neighboring channels. The FWM, along with SRS, is considered the major non-linear effect that degrades the WDM system performance [27][28]. The strength of non-linear effects based on channel parameters is explored in [29],[30] and [31]. A relationship between bitrate difference between the two channels and channel quality is proposed in [32]. It is also suggested that time shifting the interfering WDM channels may have huge impact on OSNR (6 dB in this case), since it completely changes the interference conditions and thus leads to different crosstalk-induced sensitivity degradations.

Various methods and techniques were developed to lessen the impact of FWM on transmission quality. One of them is unequal channel allocation described in [33] and [34]. Many variations of this technique were implemented with either repeated [35][36] or non-repeated channel spacings [37][38]. Another proposed way of improving transmission quality is WDM crosstalk mitigation through DSP. A method of adding a copy of the shared spectrum with a 180° difference is described in [39].

Another solution is replacing SMF with multi-core fiber, thus reducing the number of channels in a single core [40]. A method for directly measuring non-linear crosstalk through coherent optical detection is presented in [41] and the physical principles of non-linear pulse propagation are explained in [42].

2.4 Channel coexistence

I plan to focus on the interaction of an OOK modulation with more advanced modulations to represent a mixed line-rate optical network undergoing a system capacity enhancement. The crosstalk between the coexisting channels is the main concern when implementing new channels into a WDM system. As shown in [43], channels suffering from WDM crosstalk exhibit roughly 2-3 dB lower OSNR than when transmitting independently. Ref. [44] describes the impact of crosstalk on DPSK and DQPSK channels. DQPSK channels are heavily affected by interference, especially when it is caused by amplitude modulation, such as OOK channels. Even though DQPSK channels suffer the most when implemented in WDM, the overall transmission quality is still better than that of an OOK channel's. NRZ-OOK shows the worst performance among all modulation formats, with DPSK modulation being the most robust when it comes to cross-channel interference [45]. The coexistence of channels with different bitrates is discussed in [46] and [47]. In order to reduce the impact of crosstalk on transmission quality, sufficient channel spacing has to be used. In Ref. [48], channel spacing of over 75 GHz was required to reach the desired transmission quality. I suspect the channel spacing required to eliminate cross-channel interference will be higher in my case, due to FWM effects being more pronounced because of even channel spacing that I decided to use to ensure better system modularity.

Instead of simply adding new channels into an existing system in order to increase its capacity, different approach is considered in [49]. Multiplexing two OOK channels into a single DQPSK channel effectively doubles the system capacity. This approach is suitable for backbone links as the OOK channels can be demultiplexed again from the more advanced format. This method is elaborated upon in [50]. Instead of having OOK and DQPSK channels coexist, they are multiplexed into a single 8-APSK channel, thus eliminating any crosstalk between the two channels.

3 Methods

3.1 Time Domain Split-step

I used RSoft OptSim simulation program to perform the simulations. The program uses the Time Domain Split-step (TDSS) to perform the integration of the fiber propagation equation:

$$\frac{\delta A(t, z)}{\delta z} = \{L + N\} A(t, z) \quad (4)$$

where $A(t, z)$ is the optical field, L is the linear operator responsible for dispersion and other linear effects and N is the non-linear operator that accounts for the Kerr effect and other non-linear effects like SRS or pulse self-steeping.

The Split-Step integration algorithm works by applying separately L and N to $A(t, z)$ over small spans of fiber Δz . The error deriving from separating the effects of L and N goes to zero faster than $(\Delta z)^2$. L is determined in the time domain by calculating the convolution product in sampled time, which can be written as:

$$TDSS \rightarrow A_L[n] = A[n] * h[n] = \sum_{k=-\infty}^{\infty} A[k] h[n-k] \quad (5)$$

where $h(t)$ is the impulse response of the linear operator L .

The main advantage of using TDSS over other methods, such as Split-Step Fourier method (SSFM) is that it doesn't suffer from as high computational overhead and high memory usage as the fast Fourier transform (FFT) methods, which are also prone to time aliasing at the beginning and the end of each block if handled incorrectly [51].

3.2 BER

The simulation results are interpreted based on the bit error rate (BER) and Q-factors of measured optical channels. BER is the number of bit errors (N_{error}) divided by the total number of transferred bits (N_{total}):

$$BER = \frac{N_{error}}{N_{total}} \quad (6)$$

The most commonly used technique for measuring BER is direct error counting. This technique is seldom used in the simulation of optical systems, since the BER values tend to be very low and an accurate measurement would require a large amount of transferred bits, resulting in very long CPU times. Therefore, semi-analyt-

ical techniques are used as a compromise between simulation time and simulation accuracy. This means that no BER value is absolute, but rather an approximation with accuracy based on the number of simulated bits.

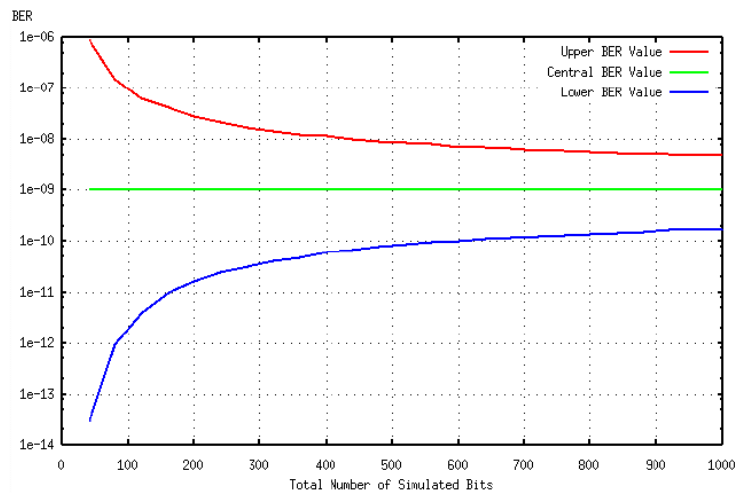


Fig. 3.1: BER estimate range (95% confidence interval) for $BER=10^{-9}$ [52].

Figure 3.1 depicts the relationship between total number of simulated bits and the BER spread. If the number of simulated bits is too low, the results may vary wildly, since each bit error will strongly affect the final BER. The improvement in accuracy becomes negligible when the number of simulated bits exceeds 800, but even then the BER value may differ by an order of magnitude.

3.3 Q-factor

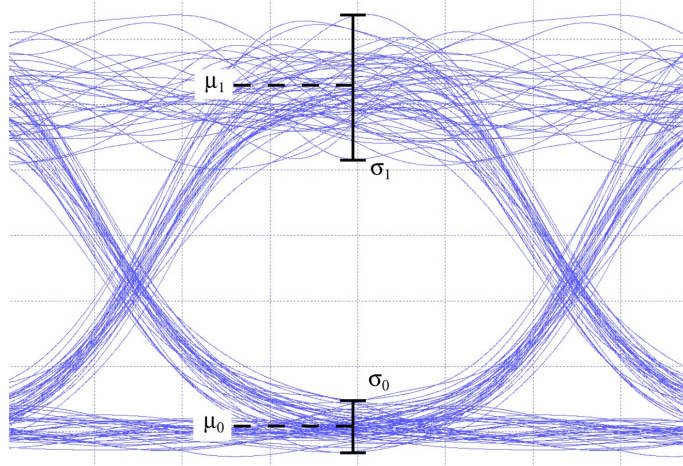


Fig. 3.2: Determining the Q-factor.

AS defined by ITU-T [53], the Q-factor is the signal-to-noise ratio at the decision circuit in voltage or current units typically expressed by:

$$Q = \frac{\mu_1 - \mu_0}{\sigma_1 + \sigma_0} \quad (7)$$

where μ_1 and μ_0 are the mean values of logical 1 and 0, σ_1 and σ_0 are their standard deviations. The Figure 3.2 illustrates where those values lie within the eye diagram.

The mathematic relations to BER when the threshold is set to optimum are:

$$BER = \frac{1}{2} \operatorname{erfc}\left(\frac{Q}{\sqrt{2}}\right) \approx \frac{1}{Q\sqrt{2\pi}} e^{-\frac{Q^2}{2}} \quad (8)$$

with:

$$\operatorname{erfc}(x) = \frac{1}{\sqrt{2\pi}} \int_x^{\infty} e^{-\frac{\beta^2}{2}} d\beta \quad (9)$$

Similarly to BER, there is an intrinsic uncertainty in the evaluation of the Q-factor when measured over a finite number of bits.

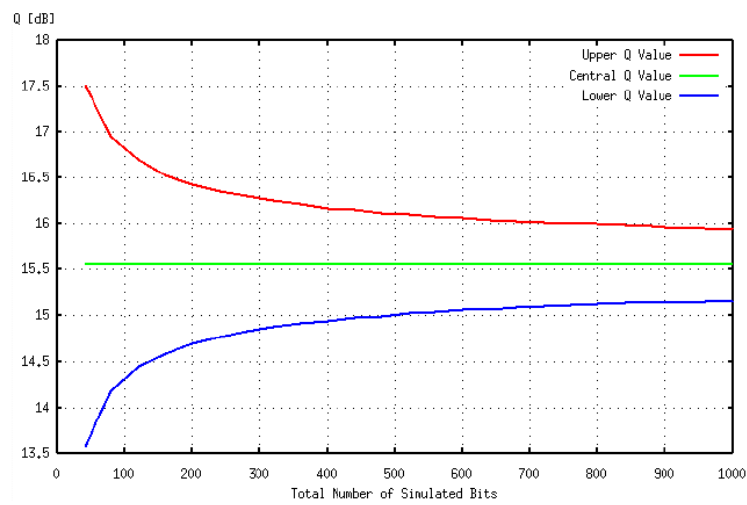


Fig. 3.3: Q-factor estimate range (95% confidence interval) for $Q=15.56$ dB, corresponding to $BER=10^{-9}$ [52].

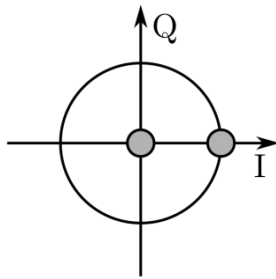
As can be seen in Fig. 3.3, approximately 500 bits are required in order to achieve Q-factor confidence intervals of less than 1 dB. Based on the relationship between the number of simulated bits and simulation accuracy for both BER and Q-factor, I decided to always simulate more than 800 bits to ensure the simulation results are reasonably accurate.

3.4 Modulations

Three modulations commonly used in optical communication systems were utilised in order to measure the interaction between different optical systems sharing a physical layer. The modulations used are Non-Return-to-Zero (NRZ) On-Off-Keying (OOK), Differential Phase-shift Keying (DPSK) and Differential Quadrature Phase-shift Keying (DQPSK).

3.4.1 NRZ-OOK

a)



b)

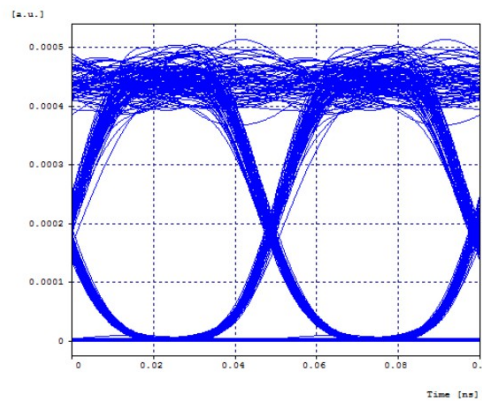


Fig. 3.4: a) OOK modulation constellation diagram, b) NRZ-OOK eye diagram

The constellation diagram of a NRZ-OOK modulation in Figure 3.4a shows the two modulation states. When looking at the eye diagram of a NRZ-OOK modulation (Fig. 3.4b), it can be seen that most of the distortion is present at logical 1 while logical 0 is relatively undistorted.

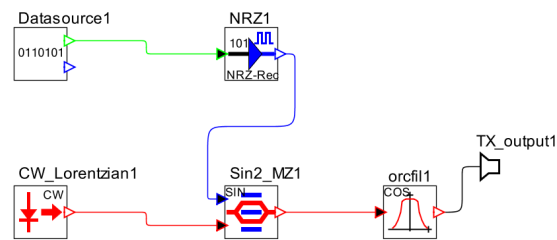


Fig. 3.5: NRZ-OOK transmitter implementation.

As depicted in Figure 3.5, it is implemented using Lorentzian laser source and Mach-Zehnder modulator. The electrical signal representing the transmitted data is modulating the optical power of the laser, thus transmitting the data as an optical signal. The signal then passes through a raised-cosine optical filter to reduce crosstalk.

3.4.2 DPSK

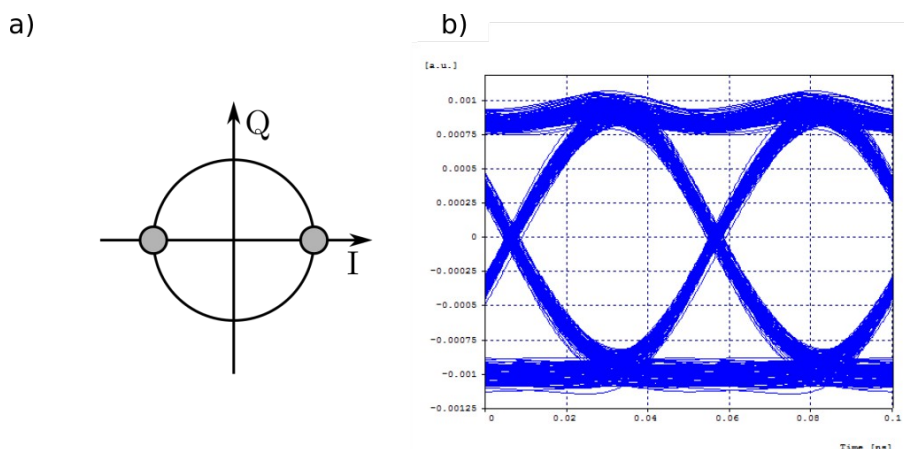


Fig. 3.6: DPSK modulation constellation diagram, b) DPSK eye diagram

Differential Phase-shift Keying is a relatively simple and robust phase modulation. Each symbol carries only one bit of information with either logical 1 at a determined phase or logical 0 at the opposite phase, resulting in very high symbol distance as can be seen on the constellation diagram in Fig. 3.6a. Since the two symbols lie on the opposite side of the constellation diagram, the eye diagram of a DPSK modulation is symmetrical along the x axis as seen in Fig. 3.6b. The main benefit of DPSK when compared to OOK modulation is the approximately 3 dB lower OSNR required to reach a given BER [54].

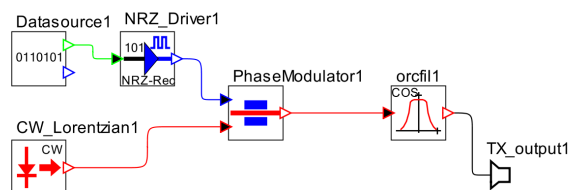


Fig. 3.7: DPSK transmitter implementation.

Instead of a Mach-Zehnder modulator present in OOK modulations, a phase modulator is used to alter the phase of a signal from Lorentzian laser source based on electrically transmitted data (Fig. 3.7). It is to be noted that the Mach-Zehnder modulator can be used as well although it has to be driven at twice the switching voltage required for OOK modulation [55].

3.4.3 DQPSK

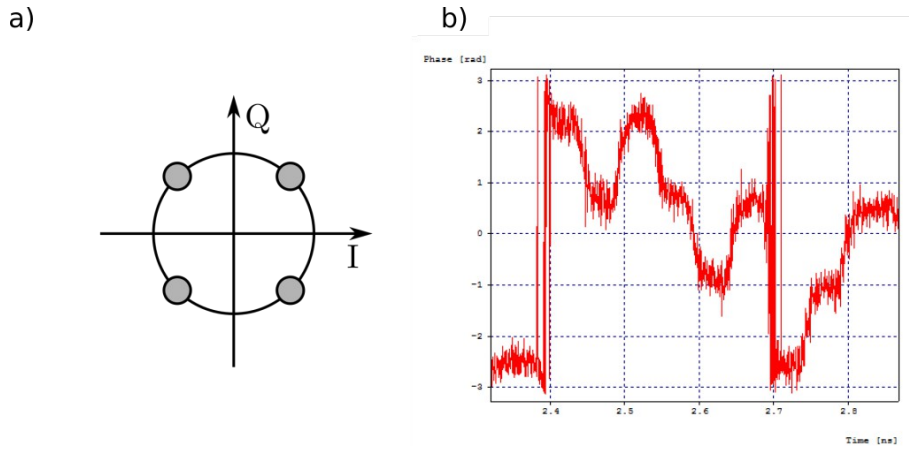


Fig. 3.8: a) (D)QPSK modulation constellation diagram, b) Instantaneous phase deviation of a DQPSK signal

Differential Quadrature Phase-shift Keying modulation differs from the two above modulations in each symbol representing two bits of information, since this phase modulation has four modulation states in total, shown in Figure 3.8a. This enables the data rate to be doubled while keeping the same symbol rate or conversely, maintain the same data rate while halving the actual symbol rate [54]. The graph in Figure 3.8b gives an example of the four phase states used to transmit data. Because all four states share the same amplitude, instantaneous phase deviation gives a better representation of the modulated signal than the eye diagram.

The implementation of a DQPSK transmitter, shown in Figure 3.9, is a bit more complicated than the implementation of other modulations. The two bit per symbol modulation is simulated by using two 1 bit data sources. After data is prepared for the modulation in the pre-coder, each data stream is sent into one of the two branches, each basically forming an independent DPSK (Differential Phase-shift Keying) modulation with one branch having its phase shifted by $\pi/2$ [56] with the help of the phase modulator.

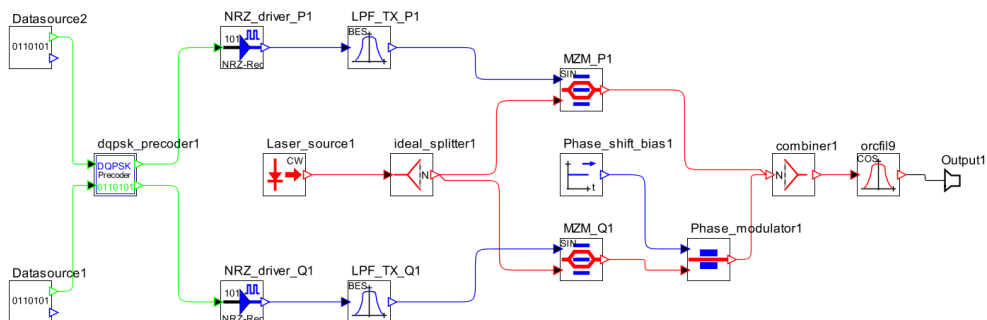


Fig. 3.9: DQPSK transmitter implementation.

3.5 Simulation layouts

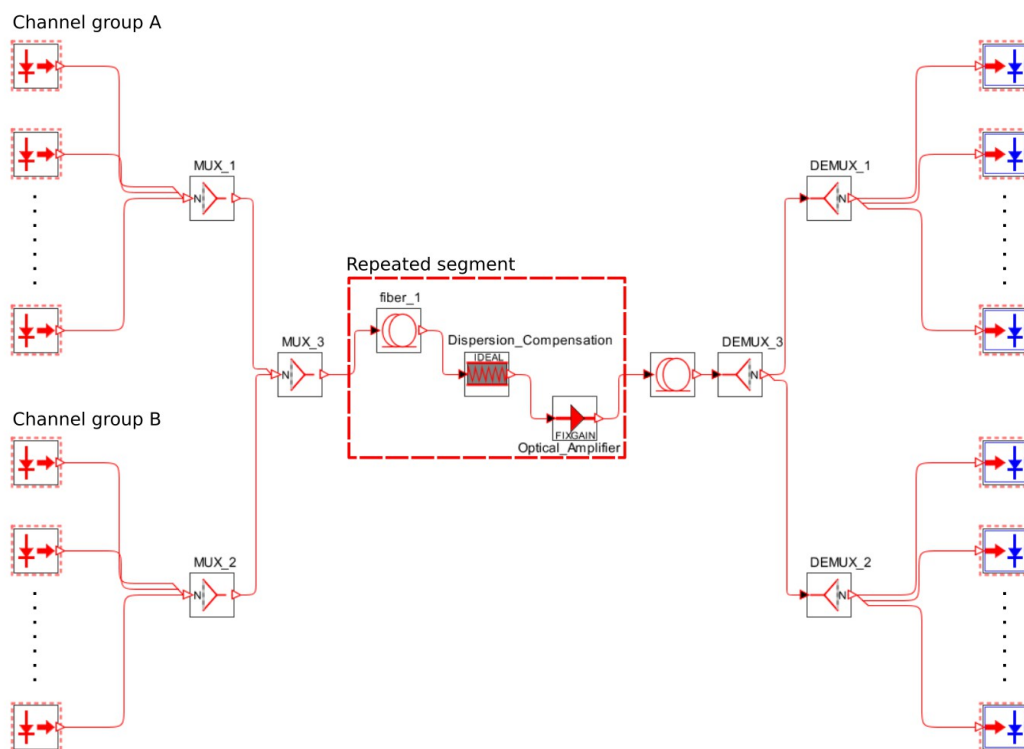


Fig. 3.10: Optical network layout with repeated signal regeneration.

Multiple simulation layouts had to be devised in order to test the interactions between optical channels. The general layout depicted in Figure 3.10 contains two DWDM systems, each consisting of ten channels. Different parameters were assigned to each system in order to observe the effect on transmission quality. The simulated network consists of several repeated segments of equal length, each containing an optical fiber, a dispersion compensation element and an erbium-doped fiber amplifier, for a total length of 300 km. The length of 300 km was chosen because it allows for a layout with several optical amplifiers in order to increase the transmission quality and because such distance is within scope of the size of Czech Republic. The fiber length in the repeated segment ranges from 50 km to 100 km based on the simulation parameters. If the length of the repeated segment was such that the total length of the system couldn't reach 300 km, the length of the final segment was adjusted to match the desired total distance. For example, if the repeated segment is 90 km long – $90+90+90 = 270$ km, it was necessary to add 30 more kilometres in order to achieve equal total length within all simulations.

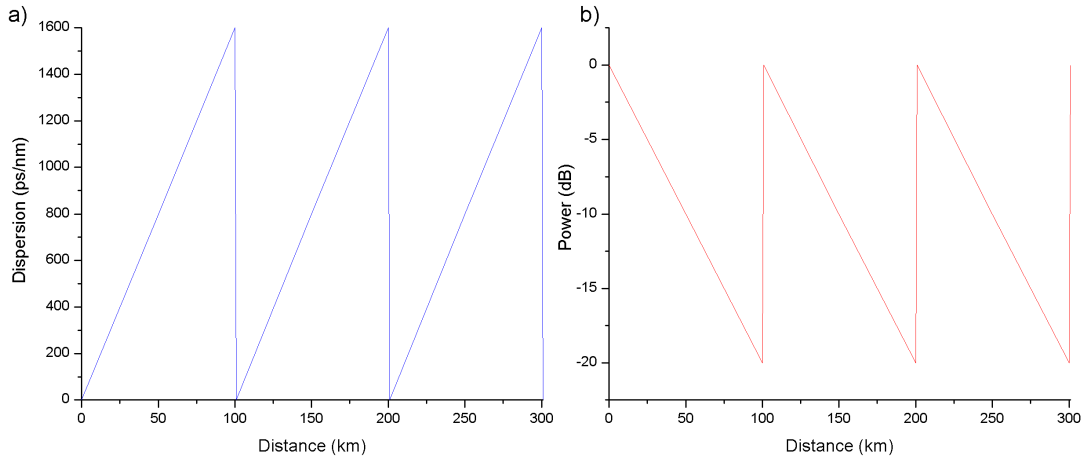


Fig. 3.11: a) Dispersion, b) power of a signal propagating through the network.

Figure 3.11 shows the dispersion and power loss compensation for signal regeneration interval of 100 km. As will be discussed in chapter 4, this regeneration interval was used in most simulations, because the reduced transmission quality from having infrequent signal regeneration allowed me to better observe the non-linear interactions between individual channels. The dispersion linearly increases at 16 ps/nm/km as the signal is propagating (Fig. 3.11a) and is fully compensated every 100 km. Similarly, the optical power steadily decreases at 0.2 dB/km until the signal reaches an optical amplifier and then is restored back to its original value. Those values for optical attenuation and dispersion were chosen to represent a typical single-mode optical fiber [11].

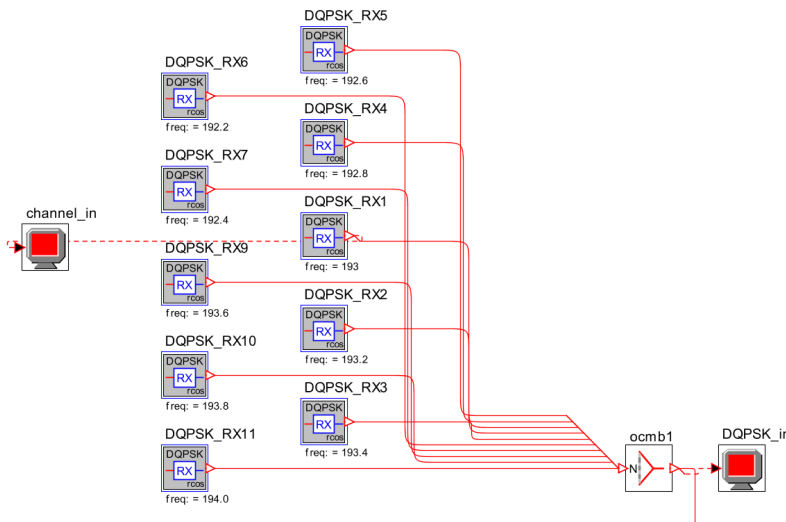


Fig. 3.12: DWDM transmitter array – DQPSK modulation.

The Figure 3.12 depicts the WDM transmitter array employed in the simulation layout. Each block contains the respective transmitter layout as described in chapter 3.4, depending on the modulation used. The channels are multiplexed using an ideal optical combiner.

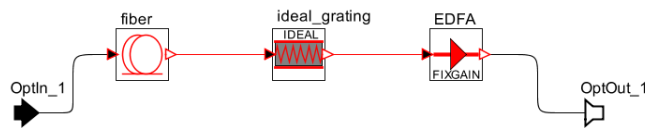


Fig. 3.13: Repeated segment with dispersion compensation and EDFA.

The repeated segment, shown in Fig. 3.13, consists of an optical fiber with length adjusted based on the simulation requirements, ideal grating for dispersion compensation and a fixed gain EDFA. Both the grating dispersion and the EDFA gain were adjusted for each simulation based on the fiber length to match the fiber dispersion characteristic and attenuation, respectively.

The WDM receiver array is shown in Fig. 3.14. As with the transmitters, each block contains a receiver layout for its respective modulation as discussed in chapter 3.4. The setup shown in the picture is specific for the DQPSK modulation receivers which have two phase-shifted outputs, requiring a more complicated detector with two inputs or two detectors with a single input. The other modulations have only a single electrical output each (blue line) so a simpler electrical detector with a single input can be used for each channel. Ideal optical splitter is used for demultiplexing.

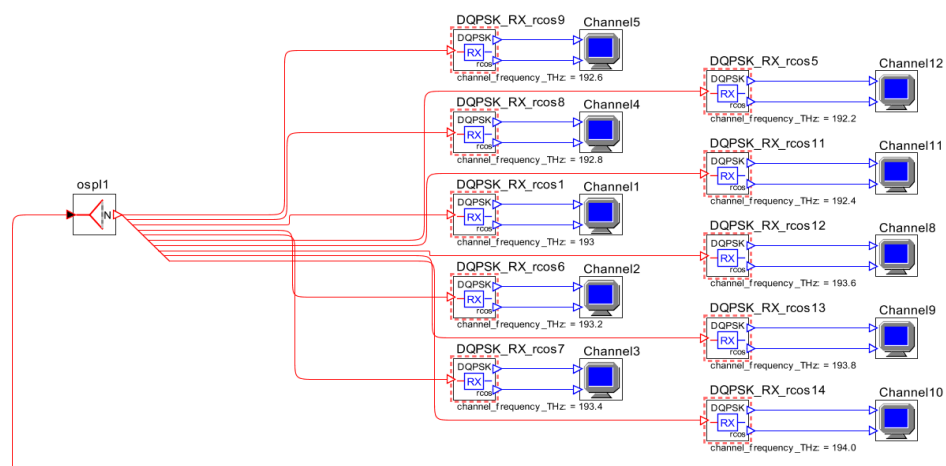


Fig. 3.14: DWDM receiver array – DQPSK modulation.

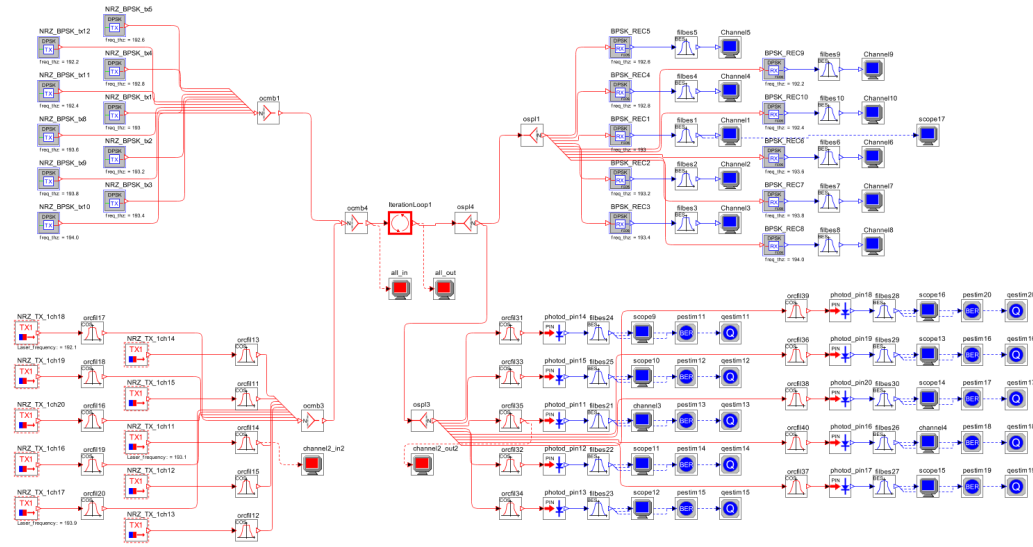


Fig. 3.15: Example of a used simulation layout – coexistence of an OOK and a DQPSK DWDM system.

The layout in Figure 3.15 is the full implementation of the general layout shown in Fig. 3.10. It consists of two transmitter arrays, each containing ten transmitters, multiplexed into a single fiber, the repeated segment represented by the block with circular arrows, and two receiver arrays with the same modulation and frequency setup as the transmitters.

4 Results

4.1 Channel properties

The purpose of this section is to design the optical network in such a way that the transmission quality is sufficient, but at the same time the bit error rate is high enough to enable further testing. In case the BER is too low, there is the risk of simulation results falling below the detection threshold. In order to set up the optical network properly, I tested the basic properties of my network components on both a simple PON layout and layout with multiple optical amplifiers.

4.1.1 Attenuation

Optical attenuation is the main limiting factor when designing an optical network. In order to reduce transmission losses, active optical components, such as Erbium-doped fiber amplifiers, have to be utilised with the drawback of introducing more noise into the system.

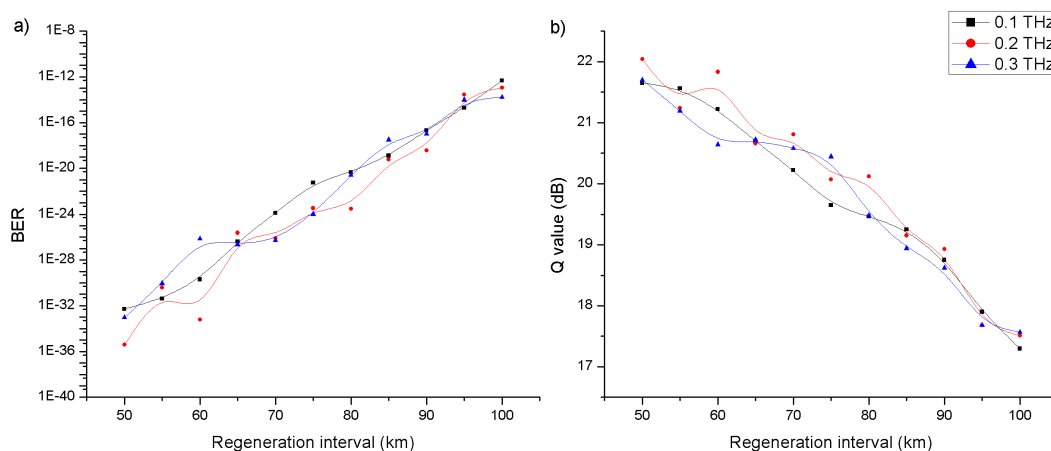


Fig. 4.1: Impact of distance between EDFA segments on a) BER, b) Q-factor

The graphs shown in Fig. 4.1 depict the results of a simulation whose purpose was to verify relationship between signal regeneration interval and transmission quality. Each graph consists of three curves which correspond to the channel spacings of 0.1, 0.2 and 0.3 THz, respectively. With the increasing distance between the individual EDFA sections the bit error rate increases (Fig. 4.1a) and the Q-factor decreases (Fig. 4.1b). Even though a larger number of optical amplifiers introduces more noise into the system, more frequent signal regeneration is clearly beneficial to the trans-

mission quality. The major real-application downside of having shorter regeneration intervals is the increased price of such system resulting from having larger amount of expensive active optical components. Irregularities with the transmission quality, which are especially apparent for channel spacings of 0.2 and 0.3 THz with more frequent signal regeneration, may be caused by greater number of optical amplifiers present which results in stronger non-linear effects. I opted for the 100 km regeneration interval for further simulations as it puts the bit error rate close to the limit for what would be considered high-quality transmission (BER of 10^{-10} according to [32]).

4.1.2 Dispersion

Unlike attenuation, dispersion can be countered with passive optical components, specifically dispersion compensating fibers or chirped Fiber Bragg Grating. I decided to use the grating for dispersion compensation, since it exhibits better compensation properties and introduces less non-linearities into the system so it won't collide with the non-linear behaviour caused by the coexistence of multiple channels that I want to focus on.

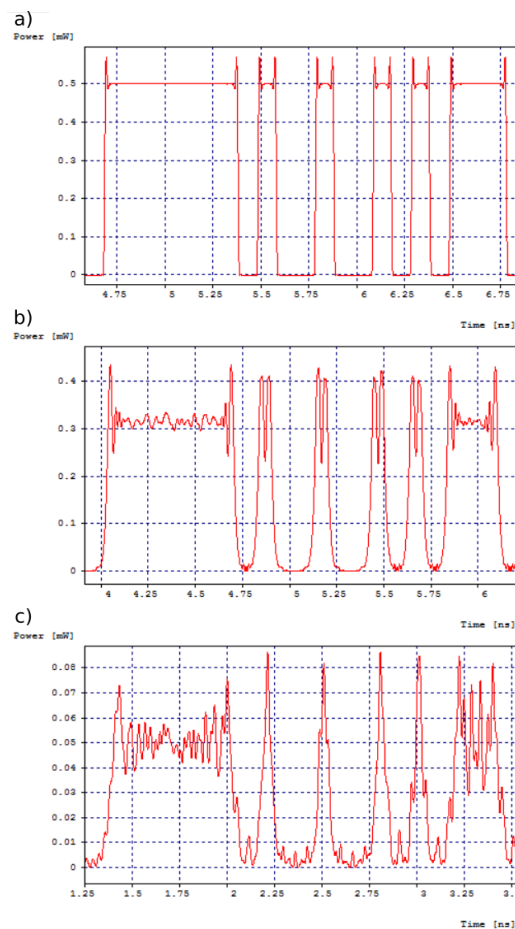


Fig. 4.2: Optical power a) transmitted, b) at 10 km, c) at 50 km.

Figure 4.2 shows the effect of dispersion (in time domain) on the optical power of a signal propagating through an optical fiber. Fig. 4.2a depicts the transmitted signal – a square pulse with steep edges and some overshoot. After 10 km, the impact of dispersion becomes apparent (Fig. 4.2b). The signal is slightly deformed, the edge steepness is decreasing and the pulses widen. At 50 km (Fig. 4.2c), the signal is heavily distorted and distortion products are forming in spaces between the pulses.

Figure 4.3 shows the reconstruction of a distorted optical signal transmitted through a 50 km long passive optical network. Accounting for dispersion allows increasing the transmission quality in long optical fibers without active network components. As I plan to make use of relatively long signal regeneration intervals in order to strain the optical system, correctly compensating the dispersion is absolutely vital.

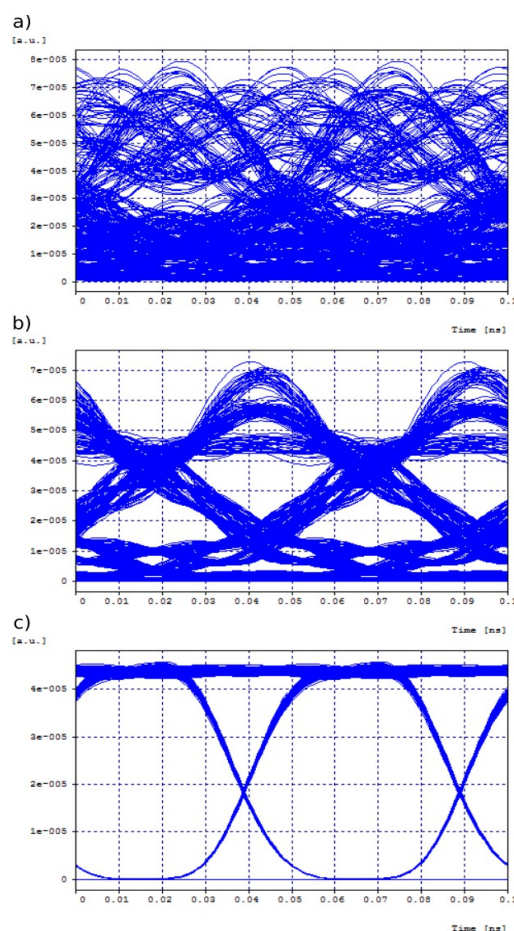


Fig. 4.3: Dispersion compensation: a) none, b) partial, c) full compensation.

4.2 Adding new channels to an existing system

When upgrading an optical network to a system with different modulation or higher bitrate, there are many things that have to be considered. In practical applications, it is generally not desirable to simply replace old channels with newer ones, since upgrading the system in such a way would result in temporary loss of service and, if any problems with the new system occurred, rollback to the old one would be problematic as well with the old channels already gone. Because of that, the upgrade is usually done in several steps. First, new channel group with the desired properties and total bit rate at least equal to the existing system is added. After the new channels are tested and ready for use, the service is switched from the old channels onto the new ones. When the new channel group is fully operational, the old system can be either discarded or replaced without any significant loss of service. This chapter explores the transitional period when two systems with different properties coexist.

4.2.1 System with mixed channel groups

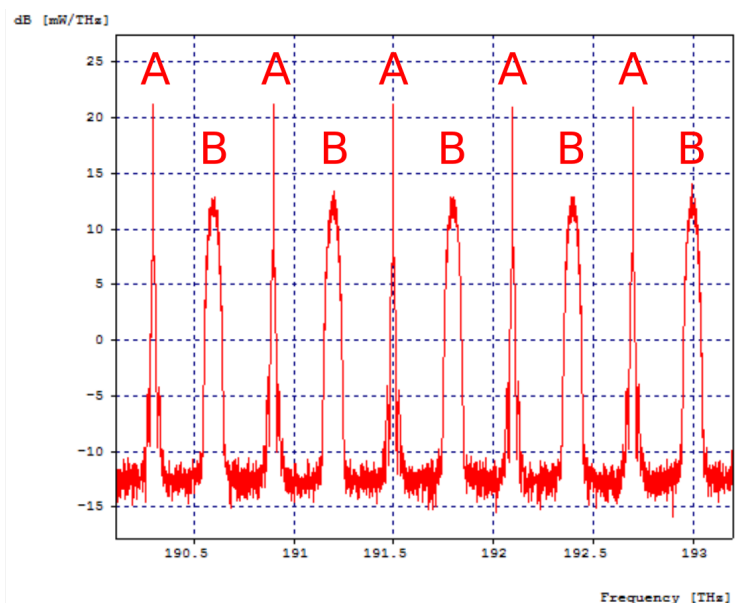


Fig. 4.4: Interleaved DWDM channels.

There are several ways of adding new channels to an existing system. One of them is putting new channels in between existing channels, provided the frequency spacing is large enough to allow it. This method is shown in Fig. 4.4. The channel group A and the channel group B, with different bit rates and modulations, are not spectrally separated but instead each channel neighbors with channels from the other group.

This chapter explores the impact of mixing channel groups on transmission quality. All simulations are made with real-life applications in mind, mostly focusing on the coexistence of a slower system with a simple modulation (typically NRZ-OOK) with a faster, more complicated system.

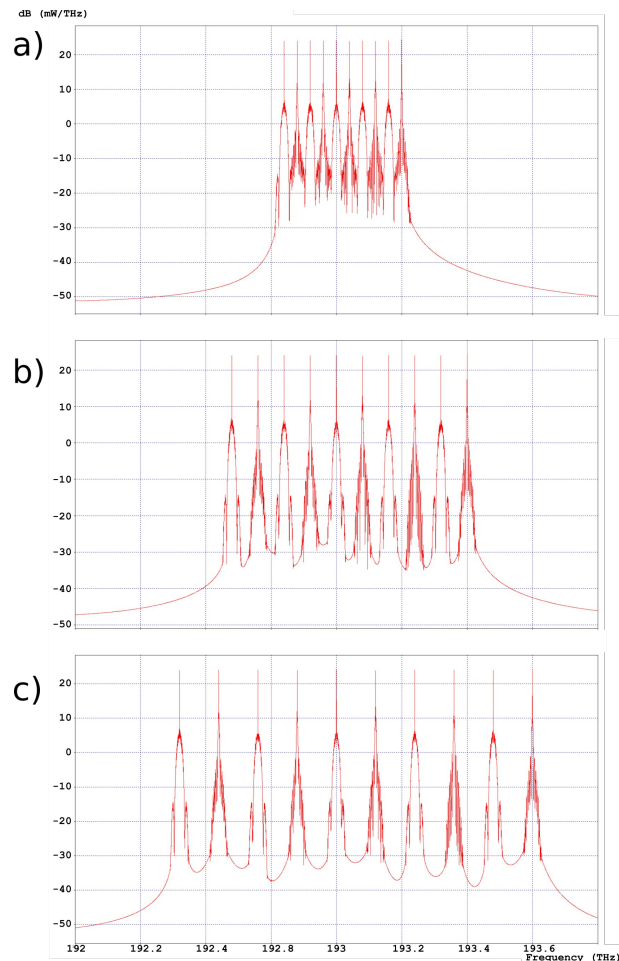


Fig. 4.5: Frequency spectrum of interleaved DWDM system.

Simulations shown in Figure 4.5 were made using the layout depicted in Figure 3.10 from chapter 3.5, making use of the NRZ-OOK (Non-Return-to-Zero On-Off Keying) modulation. This simple modulation is mainly suitable for lower bit rates [58], which resulted in lowered transmission quality for bit rates approaching 100 Gbps. Figure 4.5a, b and c represents the spectral distribution of individual DWDM channels. Three values were used for channel spacing. Spacing of 0.1 THz (Fig. 4.5a) corresponds to the defined minimum DWDM spacing. Since the channels are closely packed together, increased cross-channel interference can be expected. Two channel types can be distinguished in the graph. 10 Gbps channels with narrow spectral characteristic are interleaved with 40 Gbps channels with broader spectrum

resulting in higher amount of noise produced at the adjacent frequencies. Fig. 4.5b depicts wider spacing of 0.2 THz, spacing of 0.3 THz shown in Fig. 4.5c corresponds to the usage of every third channel on the DWDM frequency grid as described by ITU [7].

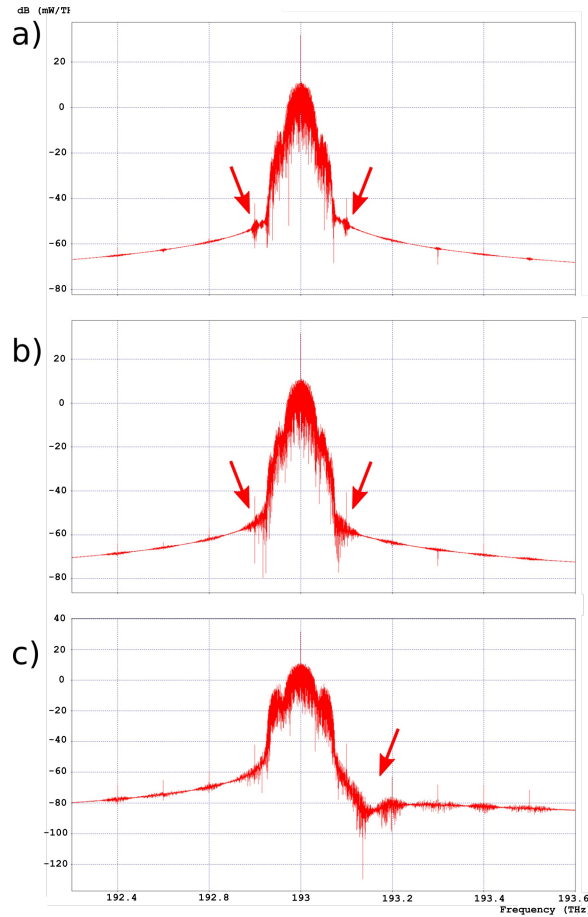


Fig. 4.6: The effects of adjacent channel interference.

Simulation described by Figures 4.6a,b and c explores the effect of adjacent channel bit rate on transmission quality of an examined 40 Gbps channel. Fig. 4.6a shows the spectral characteristic of the channel with 10 Gbps adjacent channels. We can notice two local maxima at frequencies corresponding to the adjacent channels (in this case 192.9 and 193.1 THz). This is the optical power leaking from neighboring channels through the optical filter causing interference. Increase in bit rate of the surrounding channels results in merging of those local maxima with the main spectral characteristic (Fig. 4.6b). If the bit rate is increased to 100 Gbps (Fig. 4.6c), the characteristic stops being symmetrical. Such interference can have negative impact on the bit error rate of the channel.

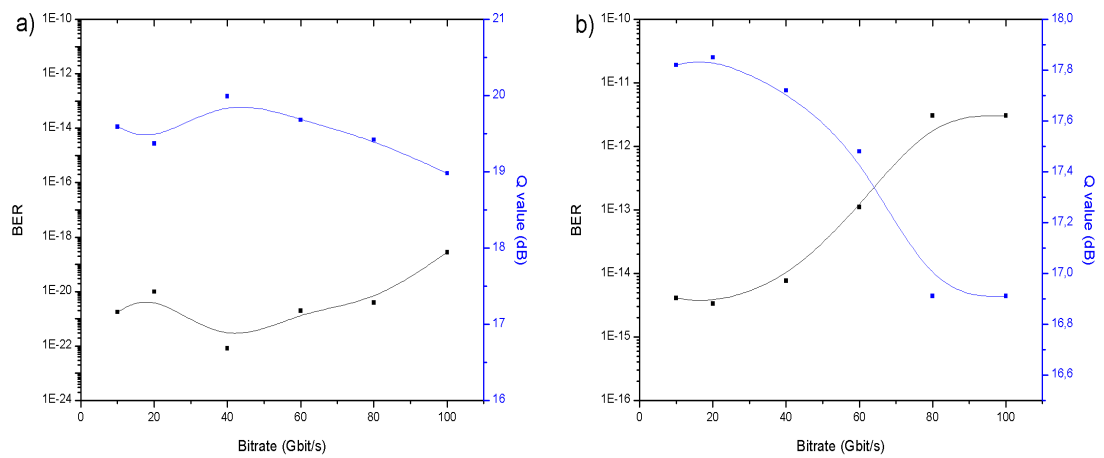


Fig. 4.7: Adjacent channel interference impact on a) 40 Gbps channel, b) 60 Gbps.

Graphs in Fig. 4.7 show the impact of adjacent channel bit rate on the error rate and Q-factor. As can be especially apparent in case of a 40 Gbps channel in Fig. 4.7a, the correlation is not linear. Fig. 4.8 shows BER of 10 different DWDM channels impacted by adjacent channel interference with a dashed line representing the BER value for a channel with no interference. Each channel exhibits strongly non-linear relationship with the interference, but the BER values don't deviate too wildly from a certain average. This means the interference can be described statistically – with an average value and a standard deviation. Because of this, all the results are based not on the properties of a single channel but on the average values of multiple channels with the same parameters.

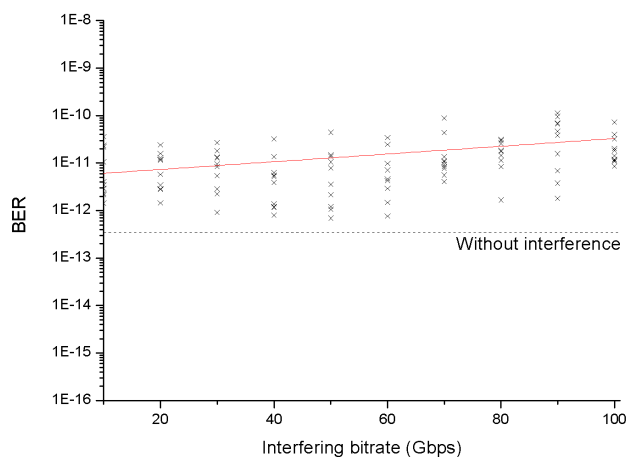


Fig. 4.8: Adjacent channel interference for 10 DWDM channels

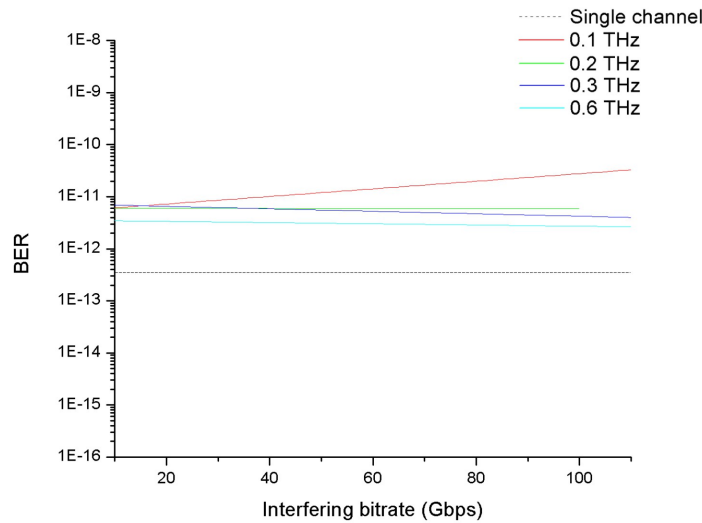


Fig. 4.9: Differences in the effect of interference based on channel spacing.

I used a 20-channel setup to evaluate the effects of adjacent channel interference. Ten evaluated channels were set up with fixed 40 Gbps bit rate, the other ten channels were used as sources of interference with variable bit rate ranging from 10 to 100 Gbps and were placed between the measured channels. Three optical amplifiers with long, 100 km gaps between them were utilised in order to push the system to its limit – if the overall BER was too low, measured interference might not be detected. Figure 4.9 contains four curves representing the average bit error rates of measured channels with various spacing and a dotted line representing a single channel with no interference as a reference value.. Channels spaced at 0.2 THz (green) and 0.6 THz (teal) show very mild increase in channel quality with higher interfering bit rate, 0.3 THz spacing (blue) results in slightly sharper sloped line fit. Channels with 0.1 THz spacing represented by the red curve differ significantly from the other three, it's the only curve showing indirect correlation between the two parameters. This means the spectral distance between channels plays an important part in the equation as it can affect not only the interference value, but also the shape of the diagram itself.

4.2.2 Interference caused by DPSK modulation

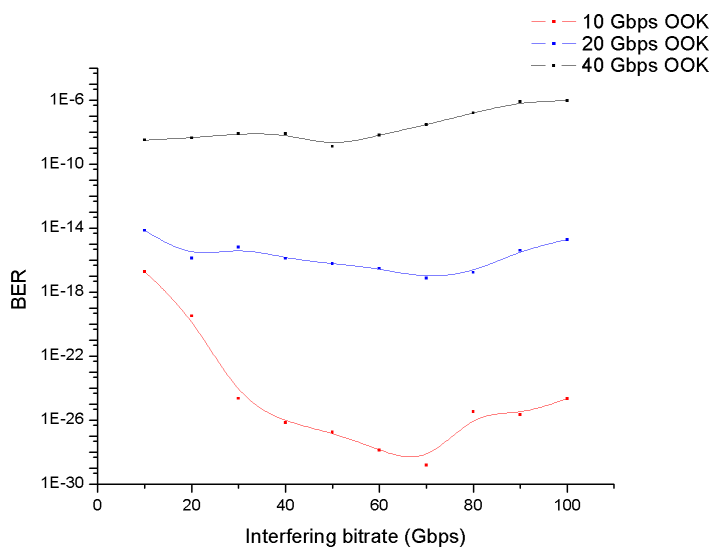


Fig. 4.10: Interference caused by DPSK channels.

Not only the channel bitrate and spacing can influence the transmission quality. Adding channels with a more advanced modulation may affect the old channels differently than expanding the system with channels using the same modulation. In this context, this section explores the impact of adding DPSK channels to an OOK system. Since the bit error rate of DPSK modulation is several magnitudes lower than the bit error rate of OOK channels, only the latter are considered when determining the crosstalk effects.

Figure 4.10 depicts the bit error rates of three OOK systems operating at channel speeds of 10, 20 and 40 Gbps while being affected by interleaved DPSK channels. 0.1 THz channel spacing was chosen for the simulation in order to maximise the effects of interference. As opposed to crosstalk from other OOK channels (as seen in Fig. 4.9), the relationship between the interfering bitrate of the DPSK channels and the OOK channels' bit error rate is non-linear, especially for low-bitrate OOK channels. If we focus on the 10 Gbps OOK curve, we can see that the crosstalk is stronger when DPSK channels operate at similar bitrates as the OOK system. This is most likely caused by each symbol being affected by a low number of interfering pulses of similar duration. If affected by multiple shorter pulses thanks to high bitrate difference, the impact of individual pulses may balance out without strongly affecting the optical power of the transferred symbol. Longer pulses affecting the whole symbol have higher chance of pushing the transferred optical power over the decision threshold resulting in increased BER.

4.2.3 Interference caused by DQPSK modulation

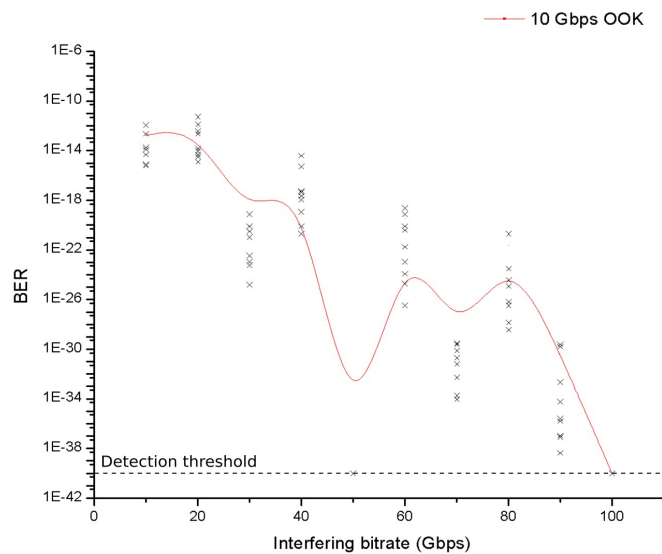


Fig. 4.11: BER of 10 Gbps OOK channels affected by DQPSK channel crosstalk.

Another modulation commonly used in optical communication systems is DQPSK. Figures 4.11 and 4.12 describe the impact of adding channels with this modulation on transmission quality of the OOK system. The Figure is split into two section for clarity, Fig. 4.11 shows how the BER of 10 Gbps OOK channels is affected and the curves in Fig. 4.12 represent the average transmission quality of 20 and 40 Gbps channels affected by DQPSK channels with bitrate ranging from 10 Gbps to 100 Gbps.

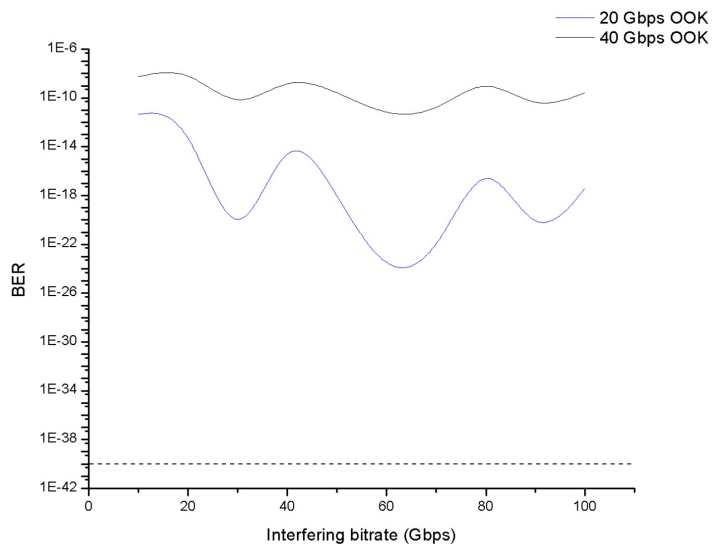


Fig. 4.12: BER of 20 and 40 Gbps OOK channels affected by DQPSK channel crosstalk.

The relationship between channel BER and interfering channel bitrate is strongly non-linear with observable similarities across all three curves. Each curve exhibits several peaks which correspond to multiples of the affected bitrate with BER decreasing as the interfering bitrate increases. In the case of 20 and 40 Gbps channels, the curves peak at 20, 40 and 80 Gbps bitrate of interfering DQPSK channels with the best transmission quality at 60 Gbps interfering bitrate. Similarly, the local maximums of 10 Gbps channel BER are located at 10, 20, 40, 60 and 80 Gbps, marking the even multiples of the channel bitrate. The lower values are present at odd multiples and high interfering bitrates, with the channel BER falling below detection threshold when confronted with 50 Gbps and 100 Gbps interference. On one hand, the interference caused by DQPSK modulation is stronger than the one caused by DPSK but on the other, DQPSK provides several bitrate “windows” allowing relatively unobstructed operation of the OOK system when configured correctly.

4.2.4 System with separated channel groups

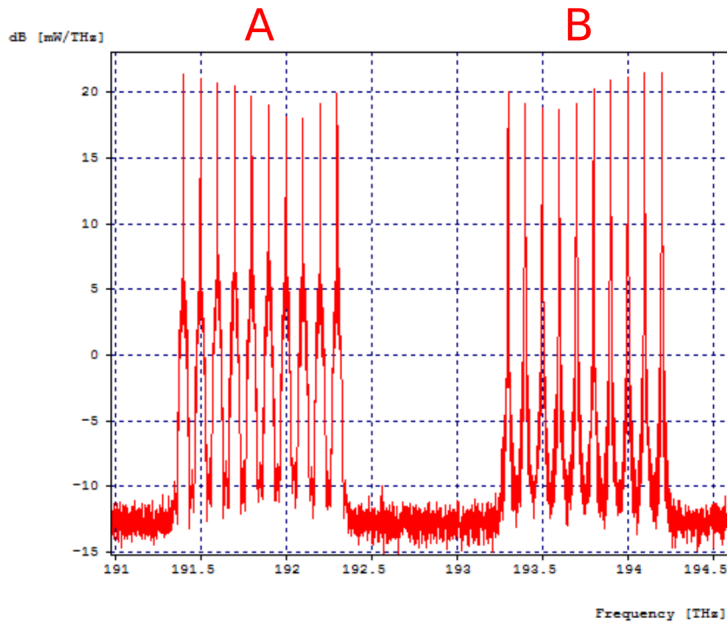


Fig. 4.13: Separated channel groups.

Next, I decided to compare the results to a network with separated channel groups, meaning channels of the same bitrate and modulation are grouped together as illustrated in Fig. 4.13, where the grouping on the left consists of 40 Gbps channels and the one on the right consists of interfering channels with variable bit rate. The fairly large frequency gap of 0.9 THz was chosen to represent systems that are relatively independent on each other. As can be seen from the fitted lines representing

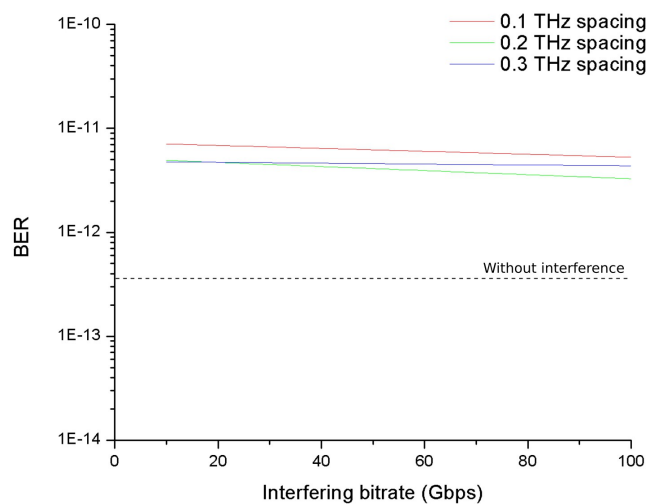


Fig. 4.15: Channel crosstalk at three different channel spacings.

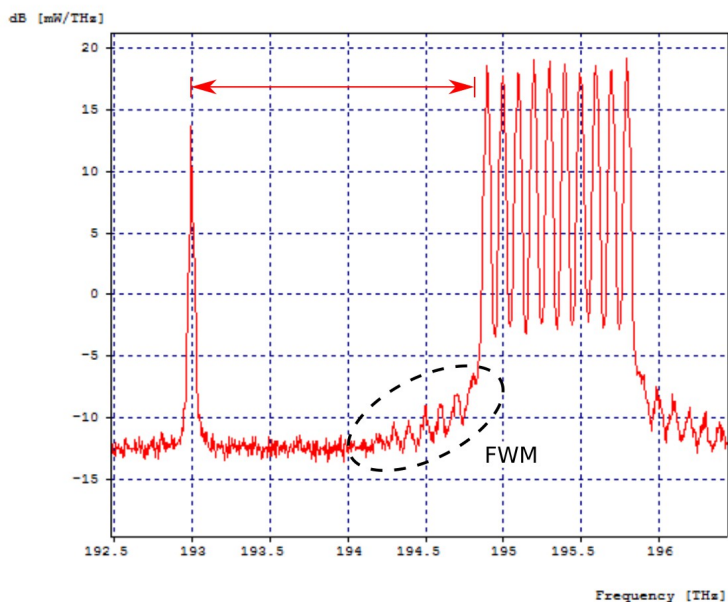


Fig. 4.14: Finding the optimal frequency spacing.

the mean BER values at 10 to 100 Gbps interfering bitrates, shown in Figure 4.15 for 0.1, 0.2 and 0.3 THz channel spacings, the impact of the interference on average transmission quality is negligible. Interference among the measured channels mainly comes from the other neighboring 40 Gbps channels and so is fairly independent from the other channel group because the varied bitrate channels are very far from the measured channels with constant 40 Gbps bitrate and thus contribute little to the cross-channel interference.

To find the optimal frequency spacing between two channel groups, I utilised the configuration explained by Fig. 4.14. The spectral distance between a single measured channel and ten interfering channels is gradually increased to find the point when the BER value of the measured channel stabilises. The effects of FWM are highlighted, forming peaks at 0.1 THz intervals and being the main source of cross-channel interference.

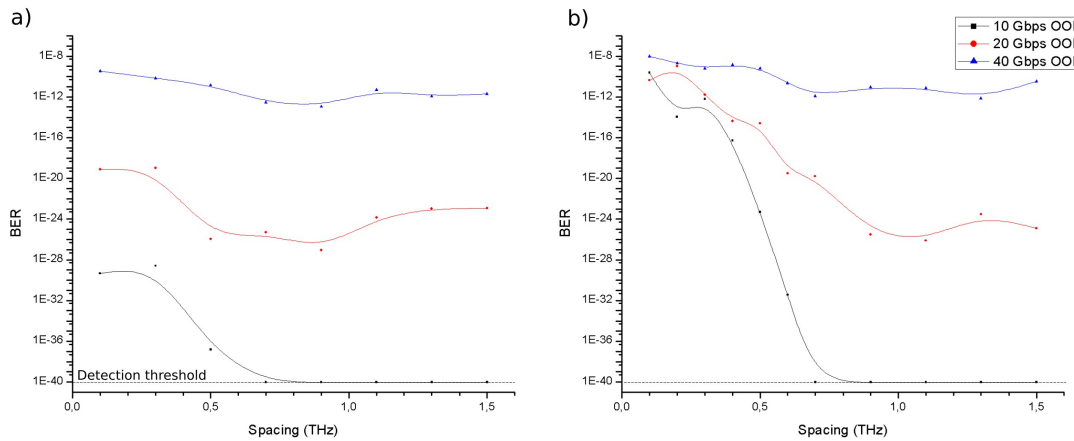


Fig. 4.16: The relationship between frequency spacing and bit error rate.

The curves in Figure 4.16 present the impact of spectral distance between the two systems on bit error rate for interference caused by DPSK (4.16a) and by DQPSK (4.16b) modulation operating at the same bitrate. Each graph consists of three sets of points representing the BER values of 10, 20 and 40 Gbps OOK channel and curves representing the overall trend for added clarity. A clear pattern can be noticed among all curves. After the spacing exceeds 0.5 THz, there is a sharp increase in transmission quality with BER even falling under the detection threshold in the case of 10 Gbps channels. The lower bitrates generally benefit more from wider spacing. This is probably the result of being less affected by noise from other sources, so the crosstalk becomes the main factor determining the error rate. Since the 40 Gbps channel signal is already heavily distorted, the added noise from inter-channel crosstalk has little effect on the overall shape of the curve. The DQPSK modulation affects the channel more than the DPSK modulation, this reflects the findings from chapter 4.2.3. The relationship between frequency spacing and BER is not linear, since there are more sources of non-linearities affecting the channel but it is safe to assume, especially when looking at the 10 Gbps channels, that the interference caused by the neighboring channel group becomes negligible with frequency spacing greater than roughly 0.7 THz.

4.2.5 Transitioning to a new system

As was discussed in previous chapters, adding new channels to an existing system affects the bitrate of the old channels. If transition is not handled properly, it can negatively impact the transmission quality during the transitional period when both new and old channels coexist.

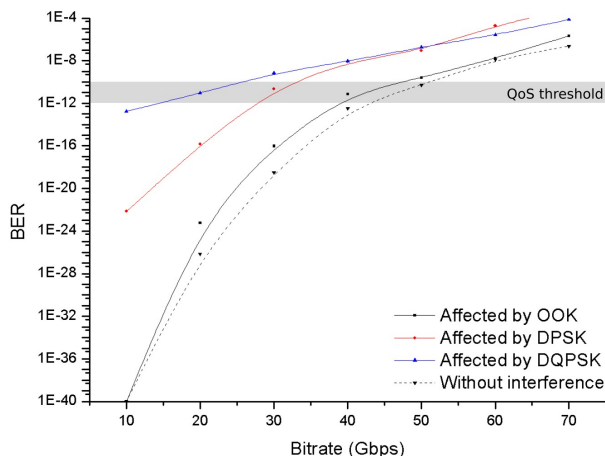


Fig. 4.17: OOK channel affected by various sources of interference.

The Figure 4.17 describes the relationship between channel bitrate and the resulting error rate. The black dashed curve represents the bit error rate of the old NRZ-OOK channels running at bitrate denoted by the x axis, before the addition of any new channels. The channel quality is suitable for lower bitrates with BER sitting just below the threshold for high quality transmission at 40 Gbps. At 50 Gbps, the bit error rate is just below 10^{-10} , if the bitrate is increased further, the BER values climb over the threshold and the quality of service (QoS) suffers. The solid black curve represents the situation when the number of channels with OOK modulation is doubled, for example when needing to increase the system capacity or to perform maintenance on the old system. The error rate is slightly higher than in previous case, but the change has little impact on the transmission quality overall. At 40 Gbps, the BER is pushed into grey zone representing the QoS threshold and at 50 Gbps, the BER value is pushed above the threshold, meaning the error rate is slightly higher than what is considered acceptable. This means that adding OOK channels to a system with channels running at speeds of 40 to 50 Gbps without making any adjustments, such as increasing the transmitting power, will have an impact on the network quality and may increase the bit error rate into levels unsuitable for communication. While the impact

on BER is relatively small in the case of adding more OOK channels, the situation changes dramatically if channels with different modulation are added instead.

The red curve shows how the OOK channels are affected by the inclusion of DPSK modulated channels. The error rate increases by several magnitudes and 40 and 50 Gbps channels become unusable. When adding DQPSK channels instead, as denoted by the blue curve, the crosstalk is further amplified with BER for a 10 Gbps OOK channel rising from below detection threshold (10^{-40}) to roughly 10^{-12} . All formerly functional OOK channels running faster than 20 Gbps become unreliable, suffering from bit error rates of above 10^{-10} .

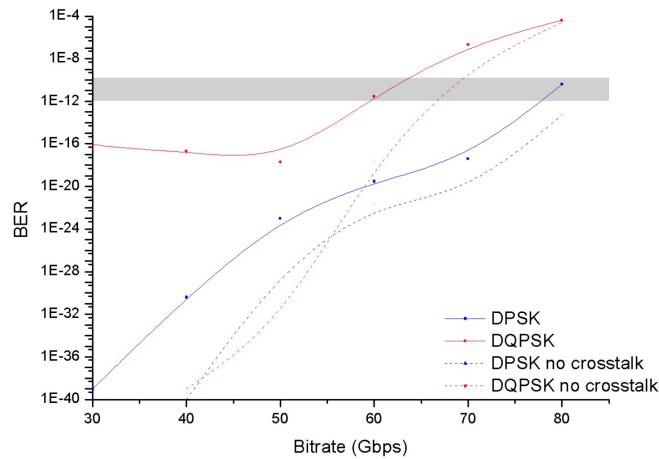


Fig. 4.18: Added channels affected by the old OOK system.

However, the OOK channels are not the only ones affected by inter-channel crosstalk. The newly added channels are affected as well. Figure 4.18 shows the impact of adding new channels, with the same bitrate as the old OOK channels, on the added channels' bit error rate. The dashed red and blue curves represent the bit error rates of DQPSK and DPSK channels unaffected by crosstalk, respectively. The solid blue curve represents the DPSK modulated channel error rate based on its bitrate. The DPSK modulation is very robust thanks to its high symbol distance. Even though BER increases by several magnitudes, the channels still manage to maintain low BER up to the bitrate of 80 Gbps where the channels start crossing the QoS threshold denoted by the grey area. The DQPSK modulation, represented by the red curve, is much more sensitive to crosstalk. While operating independently, the error rate of the DQPSK modulated channels is below the detection threshold when running at bitrates of 40 Gbps or less. When exposed to the OOK modulated channels, however, the transmission quality decreases sharply and BER reaches the QoS

threshold at 60 Gbps. Even though in this case, DQPSK channels manage to operate at higher bitrates than the OOK modulated channels described in Fig. 4.17, they are clearly much more susceptible to crosstalk. The only reason the channels manage to maintain higher transmission quality is because their parameters were deliberately set up in a way to make the addition into an OOK system possible. If both the OOK system and the DQPSK system operated at the same bit error rate independently, after forcing them to coexist on the same physical layer, the DQPSK channels' bitrate would be much lower than their amplitude modulated counterparts'.

5 Conclusion

In this thesis I explored the conditions for the coexistence of optical systems on a physical layer. First, the relationship between the length of the signal regeneration interval and transmission quality was verified, showing that the benefits of having shorter regeneration interval outweigh the negatives, even though utilising more ED-FAs introduces more noise into the system.

Then, the interactions between channels in a DWDM system were explored. The simulations show that the channel bit error rate is not only determined by the channel parameters, but by the neighboring channels' parameters as well. Interestingly, neighboring channel bitrate can have strong impact on the channel bitrate, especially if they don't share the same modulation format. As shown in chapters 4.2.2 and 4.2.3, NRZ-OOK channel BER may fluctuate when surrounded by phase-modulation channels based on the surrounding channels' bitrate. This phenomenon is most apparent in channels with very low BER, as the channel BER approaches the QoS threshold, the impact of neighboring channel bitrate becomes less noticeable.

Channel spacing also plays an important role in reducing the cross-channel interference. Simulations in chapter 4.2.4 show that there is a strong correlation between the interference caused by crosstalk and FWM and the channel spacing. In my case, a DWDM system of ten channels with 0.1 THz channel spacing noticeably affects channels up to 0.5 – 0.7 THz away from the channel group. When wanting to add another DWDM channel group, this helps us determine the optimal spacing between the two channel groups.

It was also shown that adding new channels into an optical network has a strong impact on the already present channels. Phase-modulation channels are generally affected more by cross-channel interference than the amplitude-modulated channels, but the NRZ-OOK channels suffer from lower overall performance, meaning that even though they are less affected by the addition of new channels, their performance tends to be the system's limiting factor nonetheless.

To summarise the results: when upgrading an optical network in order to increase its total bitrate, it is important to pay attention to cross—channel interactions. If the transition is done incorrectly, the network operator may lock himself in a situation where the addition of new channels would push the old OOK channels over the QoS

threshold, making the transition impossible without loss of service or adjusting the channel BER in other way, such as increasing the transmitting power, which may not be always possible.

When deciding how to add new channels, both channel interleaving and separated channel groups seem to be viable approaches. Separating the channels with different modulation formats seems to be the generally safer approach, as the cross-channel interference is strongest between channels with different modulation formats.

With regards to the results covered in this chapter, I consider the goals of this thesis fulfilled. The possible limitation of the thesis is the inherent inaccuracy of the simulations and the closed-source nature of the simulation program, meaning that the results should be verified experimentally. The possible follow-ups on this thesis may include performing an experimental analysis of the results or expanding on the scope of the thesis by for example including more modulation formats, or focusing on a specific aspect touched by the thesis, such as the BER fluctuation based on a neighboring channel bitrate.

Bibliography

- [1] G. Raybon and P. J. Winzer, "*100 Gb/s challenges and solutions*," OFC/NFOEC 2008 - 2008 Conference on Optical Fiber Communication/National Fiber Optic Engineers Conference, San Diego, CA, 2008, pp. 1-35.
- [2] A. Nag, M. Tornatore and B. Mukherjee, "*Energy-efficient and cost-efficient capacity upgrade in mixed-line-rate optical networks*," in IEEE/OSA Journal of Optical Communications and Networking, vol. 4, no. 12, pp. 1018-1025, Dec. 2012.
- [3] C. A. Brackett, "*Dense wavelength division multiplexing networks: principles and applications*," in IEEE Journal on Selected Areas in Communications, vol. 8, no. 6, pp. 948-964, Aug 1990.
- [4] K. McCammon and S. W. Wong, "*Capacity Enhancement and System Demonstration of a WDM-capable G-PON compliant to ITU-T G.984.5*," OFC/NFOEC 2008 - 2008 Conference on Optical Fiber Communication/National Fiber Optic Engineers Conference, San Diego, CA, 2008, pp. 1-5.
- [5] Agrawal, G.P., "*Lightwave Technology: Telecommunication Systems*," Wiley-Interscience, 2005
- [6] ITU-T Recommendation ITU-T G.694.2 (2012), "*Spectral grids for WDM applications: CWDM frequency grid*."
- [7] ITU-T Recommendation ITU-T G.694.1 (2012), "*Spectral grids for WDM applications: DWDM frequency grid*."
- [8] Fiberstore, "*From O to L: the Evolution of Optical Wavelength Bands*," available from: <https://community.fs.com/blog/from-o-to-l-the-evolution-of-optical-wavelength-bands.html>
- [9] J. M. Kahn and Keang-Po Ho, "*Spectral efficiency limits and modulation/detection techniques for DWDM systems*," in IEEE Journal of Selected Topics in Quantum Electronics, vol. 10, no. 2, pp. 259-272, March-April 2004.
- [10] M. Asvial and A. A. S. Paramitha M. P, "*Analysis of high order dispersion and non linear effects in fiber optic transmission with Non Linear Schrodinger Equation model*," 2015 International Conference on Quality in Research (QiR), Lombok, 2015, pp. 145-150.
- [11] Corning, "*SMF-28 Optical Fiber*," available from: <http://ece466.groups.et.byu.net/notes/smf28.pdf>
- [12] Draka Communications, "*Single-Mode Optical Fiber*," available from: https://www.prysmiangroup.com/api/product_attachment?pdf=8150

- [13] M. Lucki, T. Zeman, "*Dispersion Compensating fibers for fiber Optic Telecommunication Systems*," Advances in Optical Fiber Technology, IntechOpen, 2015
- [14] G. E. Kohnke et al., "*Fiber Bragg gratings for dispersion compensation*," Optical Fiber Communication Conference and Exhibit, 2002, pp. 578-580.
- [15] L. Čepa, M. Lucki, J. Hájek, "*Comparison of Chromatic Dispersion Compensation Methods in Conventional Single-mode Fiber*," České vysoké učení technické v Praze, FEL, 2010
- [16] G. Brochu et al., "*Channelized fiber Bragg gratings for inline chromatic dispersion compensation of 40 Gb/s links on ITU-50 grid*," 2011 37th European Conference and Exhibition on Optical Communication, Geneva, 2011, pp. 1-3.
- [17] T. He, L. Rishøj, J. Demas and S. Ramachandran, "*Dispersion compensation using chirped long period gratings*," 2016 Conference on Lasers and Electro-Optics (CLEO), San Jose, CA, 2016, pp. 1-2.
- [18] N. M. Yusoff, N. M. Sharif, A. H. Sulaiman and M. A. Mahdi, "*Investigation on the signal performances of pre-, post- and inline compensation of l-band dispersion compensator using Chirped Fiber Bragg grating*," 2015 1st International Conference on Telematics and Future Generation Networks (TAFGEN), Kuala Lumpur, 2015, pp. 107-110.
- [19] M. Movassaghi, M. K. Jackson, V. M. Smith and W. J. Hallam, "*Noise figure of erbium-doped fiber amplifiers in saturated operation*," in Journal of Lightwave Technology, vol. 16, no. 5, pp. 812-817, May 1998.
- [20] B. Zhu et al., "*Transmission of 200Gb/s PM-16QAM and 150Gb/s PM-8QAM DWDM Signals over Long-haul and Transoceanic Distance at 100km Span Length with EDFA-only*," 2017 European Conference on Optical Communication (ECOC), Gothenburg, Sweden, 2017, pp. 1-3.
- [21] J. R. Stimple, "*Testing Erbium-Doped Fiber Amplifiers*," The Hewlett-Packard Journal Article 12, 1997.
- [22] Y. Kawaguchi and T. Tsuritani, "*Ultra-long-haul multicore fiber transmission over 5,000 km using cladding pumped seven-core EDFA*," 2017 Opto-Electronics and Communications Conference (OECC) and Photonics Global Conference (PGC), Singapore, 2017, pp. 1-2.
- [23] A. W. Setiawan Putra, M. Yamada, H. Tsuda and S. Ambran, "*Theoretical Analysis of Noise in Erbium Doped Fiber Amplifier*," in IEEE Journal of Quantum Electronics, vol. 53, no. 4, pp. 1-8, Aug. 2017.

- [24] R. Ibrahim, Y. Gottesman, B. E. Benkelfat and Q. Zou, "*EDFA gain stabilization with fast transient behavior by use of a semiconductor optical amplifier*," 2007 Conference on Lasers and Electro-Optics (CLEO), Baltimore, MD, 2007, pp. 1-2.
- [25] HODŽIĆ, A. "*Investigations of high bit rate optical transmission systems employing a channel data rate of 40 Gb/s*." Doctoral thesis, Technischen Universität Berlin. Berlin, 2004
- [26] K. O. Hill, D. C. Johnson, B. S. Kawasaki, and R. I. MacDonald. "*CW three-wave mixing in single-mode optical fibers*." Journal of Applied Physics, 49(10):5098–5106, October 1978.
- [27] F. Z. El-Halafawy, M. H. Aly and M. A. A. El-Bary, "*Four-Wave Mixing Crosstalk in DWDM Optical Fiber Systems*," Proceedings of the Twenty Third National Radio Science Conference (NRSC'2006), Menoufiya, 2006, pp. 1-6.
- [28] J. Šajgalíková, J. Litvik and M. Dado, "*Simulation of FWM effects in WDM systems with various modulation formats*," 2016 ELEKTRO, Strbske Pleso, 2016, pp. 92-95.
- [29] A. Carbó, J. Renaudier, P. Tran and G. Charlet, "*Experimental analysis of non linear tolerance dependency of multicarrier modulations versus number of WDM channels*," 2016 Optical Fiber Communications Conference and Exhibition (OFC), Anaheim, CA, 2016, pp. 1-3.
- [30] A. H. Shafie, T. M. Bazan and K. M. Hassan, "*The effect of FWM and SRS on the performance of WDM systems with optical amplifiers*," 2018 35th National Radio Science Conference (NRSC), Cairo, Egypt, 2018, pp. 425-432.
- [31] M. Secondini, E. Forestieri and G. Prati, "*Achievable Information Rate in Nonlinear WDM Fiber-Optic Systems With Arbitrary Modulation Formats and Dispersion Maps*," in Journal of Lightwave Technology, vol. 31, no. 23, pp. 3839-3852, Dec.1, 2013.
- [32] P. J. Winzer, M. Pfennigbauer and R. J. Essiambre, "*Coherent crosstalk in ultradense WDM systems*," in Journal of Lightwave Technology, vol. 23, no. 4, pp. 1734-1744, April 2005.
- [33] F. Forghieri, R. W. Tkach, A. R. Chraplyvy and D. Marcuse, "*Reduction of four-wave mixing crosstalk in WDM systems using unequally spaced channels*," in IEEE Photonics Technology Letters, vol. 6, no. 6, pp. 754-756, June 1994.
- [34] A. Rouf and M. S. Islam, "*A new approach of unequally spaced channel allocation for FWM crosstalk suppression in WDM transmission system*," 2012 7th International Conference on Electrical and Computer Engineering, Dhaka, 2012, pp. 35-38.

- [35] Kwong, W. C. and Yang, G. C., "*An algebraic approach to the unequal spaced channel-allocation problem in WDM lightwave systems*," IEEE Trans. Commun. vol. 45, no. 3, pp. 352-359, 1997.
- [36] Zhang, J. G. and Sharma, A.B., "*Fast frequency allocation in WDM systems with unequally spaced channels*," Journal of Electronics Letters, vol. 39, no. 5, pp. 450-452, 2003.
- [37] Jumpates, A., Rachnarong, V. and Noppanakeepong, S., "*The Analysis of Paired Unequally Spaced Repeated Alternate Unequally Spaced Allocation Channels for FDM Lightwave System*," PIERS Proceedings, Suzhou, China, pp. 754-758, 2011.
- [38] Nagatani, Y., Ito, Y., Onishi, J., Kojima, S. and Numai, T, "*Theoretical Analysis of Frequency Allocations in FDM Lightwave Transmission Systems*." Journal of Lightwave Technology, vol. 26, no. 13, pp. 1993-2001, 2008.
- [39] M. Ziyadi et al., "*Tunable ROADM with crosstalk reduction for overlapped 20–25 Gbaud QPSK WDM channels using wave mixing*," 2016 Conference on Lasers and Electro-Optics (CLEO), San Jose, CA, 2016, pp. 1-2.
- [40] M. Arikawa, T. Ito, E. Le Taillandier de Gabory and K. Fukuchi, "*Crosstalk Reduction With Bidirectional Signal Assignment on Square Lattice Structure 16-Core Fiber Over WDM Transmission for Gradual Upgrade of SMF-Based Lines*," in Journal of Lightwave Technology, vol. 34, no. 8, pp. 1908-1915, April 15, 2016.
- [41] M. Reimer, A. Borowiec, X. Tang, C. Laperle and M. O'Sullivan, "*Direct measurement of nonlinear WDM crosstalk using coherent optical detection*," IEEE Photonics Conference 2012, Burlingame, CA, 2012, pp. 322-323.
- [42] Y. Kodama and A. Hasegawa, "*Nonlinear pulse propagation in a monomode dielectric guide*," in IEEE Journal of Quantum Electronics, vol. 23, no. 5, pp. 510-524, May 1987.
- [43] K. F. George, T. M. Bazan, S. Ghoniemy and E. S. A. El-Badawy, "*Twelve-40 Gb/s WDM communication network with different modulation formats*," 2009 6th International Symposium on High Capacity Optical Networks and Enabling Technologies (HONET), Alexandria, 2009, pp. 184-188.
- [44] L. G. C. Cancela, J. L. Rebola and J. J. O. Pires, "*DQPSK error performance in the presence of in-band interferers with different modulation formats*," 2014 19th European Conference on Networks and Optical Communications - (NOC), Milano, 2014, pp. 13-17.
- [45] H. Song and M. Brandt-Pearce, "*A Discrete-Time Polynomial Model of Single Channel Long-Haul Fiber-Optic Communication Systems*," 2011 IEEE International Conference on Communications (ICC), Kyoto, 2011, pp. 1-6.

- [46] Z. Zhang et al., "*40-Gb/s downstream and 10-Gb/s upstream long-reach WDM-PON employing remotely pumped EDFA and self wavelength managed tunable transmitter*," 9th International Conference on Communications and Networking in China, Maoming, 2014, pp. 280-283.
- [47] C. Furst et al., "*Analysis of Crosstalk in Mixed 43 Gb/s RZ-DQPSK and 10.7 Gb/s DWDM Systems at 50 GHz Channel Spacing*," OFC/NFOEC 2007 - 2007 Conference on Optical Fiber Communication and the National Fiber Optic Engineers Conference, Anaheim, CA, 2007, pp. 1-3.
- [48] A. Udalcovs, P. Monti, V. Bobrovs, R. Schatz, L. Wosinska and G. Ivanovs, "*Spectral and energy efficiency considerations in mixed-line rate WDM networks with signal quality guarantee*," 2013 15th International Conference on Transparent Optical Networks (ICTON), Cartagena, 2013, pp. 1-7.
- [49] V. Vercesi, N. Sambo, M. Scaffardi, F. Cugini, A. Bogoni and P. Castoldi, "*Routing and Optical Multiplexing of 10-Gb/s OOK Streams to (DP)-DQPSK Traffic Trunks*," in IEEE Photonics Technology Letters, vol. 26, no. 12, pp. 1176-1179, June15, 2014.
- [50] A. Malacarne, S. Pinna and A. Bogoni, "*Optical multiplexing of asynchronous OOK and DQPSK signals in PPLN waveguide*," OFC 2014, San Francisco, CA, pp. 1-3.
- [51] Y. Zhu and D. V. Plant, "*Optimal Design of Dispersion Filter for Time-Domain Split-Step Simulation of Pulse Propagation in Optical Fiber*," in Journal of Lightwave Technology, vol. 30, no. 10, pp. 1405-1421, May15, 2012.
- [52] RSoft Design Group Inc., "*Optsim User Guide*." USA, 2008
- [53] ITU-T Recommendation ITU-T G.976 (2014), "*Test methods applicable to optical fiber submarine cable systems*."
- [54] P. J. Winzer and R. J. Essiambre, "*Advanced Optical Modulation Formats*," in Proceedings of the IEEE, vol. 94, no. 5, pp. 952-985, May 2006.
- [55] A. H. Gnauck and P. J. Winzer, "*Optical phase-shift-keyed transmission*," in Journal of Lightwave Technology, vol. 23, no. 1, pp. 115-130, Jan. 2005.
- [56] R. A. Griffin and A. C. Carter, "*Optical differential quadrature phase-shift key (oDQPSK) for high capacity optical transmission*," Optical Fiber Communication Conference and Exhibit, 2002, pp. 367-368.
- [57] ITU-T Recommendation ITU-T G.652 (2016), "*Characteristics of a single-mode optical fiber and cable*."
- [58] Y. H. Wen and K. M. Feng, "*A Simple NRZ-OOK to PDM RZ-QPSK Optical Modulation Format Conversion by Bidirectional XPM*," in IEEE Photonics Technology Letters, vol. 27, no. 9, pp. 935-938, May1, 1 2015.